MASTER'S THESIS

Synthesis of Layered Double Hydroxide-Reduced Graphene Oxide Composite for Catalysis of CO$_2$ Electro-Reduction

Department of Chemistry

University of Turku
Finland
2021

Author: Wenquan Chen		
Title of thesis: Synthesis of layered double hydroxide-reduced graphene oxide composite for Catalysis of CO_2 Electro-Reduction		
Degree programme: MDP in Physical and Chemical Sciences		
Major: Materials Chemistry		
Supervisor: Dr. Lokesh Kesavan		
Date: 28.4.2021	**Number of page:** 44	**Language:** English

Abstract

CO_2 is the major component contributing to greenhouse effect that leads to global warming, rise of sea level and climate change. So recycling the content of CO_2 at atmosphere is considered to be a promising method for sustainability. Meanwhile, electrochemical conversion of CO_2 contributes to convert CO_2 into a carbon feedstock, such as CO, which can both solve the problem of environmental threat and energy preservation. But demanding part is that CO_2 is one of the most stable carbon-based molecule and high overpotential (-1.9 V) is needed for single electron reduction of CO_2. To accomplish this goal, the introduction of an effective catalyst is crucial. In this thesis, synthesis, characterization and application of layered double hydroxide-reduced graphene oxide composite (LDH-rGO) for CO_2 reduction were discussed. We are aware that LDH showed a positive catalytic activity in variety of reactions from the previous reported works. However, the bottlenecks of LDH were low electrical conductivity and low specific surface areas. In this present study, we combined LDH with rGO that possess high electrical conductivity and specific areas to form LDH-rGO composite. These materials were proven to lower CO_2 reduction potential (-1.3 V) and exhibit high current response.

Keywords: CO_2 electro-reduction, LDH, graphene, LDH-rGO, FT-IR, Cyclic voltammetry.

Table of Contents

1 Introduction

1.1 Challenges in renewable energy and global warming

Currently, fossil fuels (coal, crude oil, nature gas) still dominate the energy consumption (Figure 1) and with the development of society and economic growth, it has been predicted that the consumption of fossil fuel in the following decades will be more and more, although the proportion of green energies such as nuclear, hydro and renewables increase gradually every year. However, coal, oil and gas are all finite and non-renewable energy source, they will finally dry up in some day. L. A. Arias and colleagues [1] estimated that coal remained can be used for only 114 years, while oil and gas remain less and can only be used 50.7 years and 52.8 years, respectively.
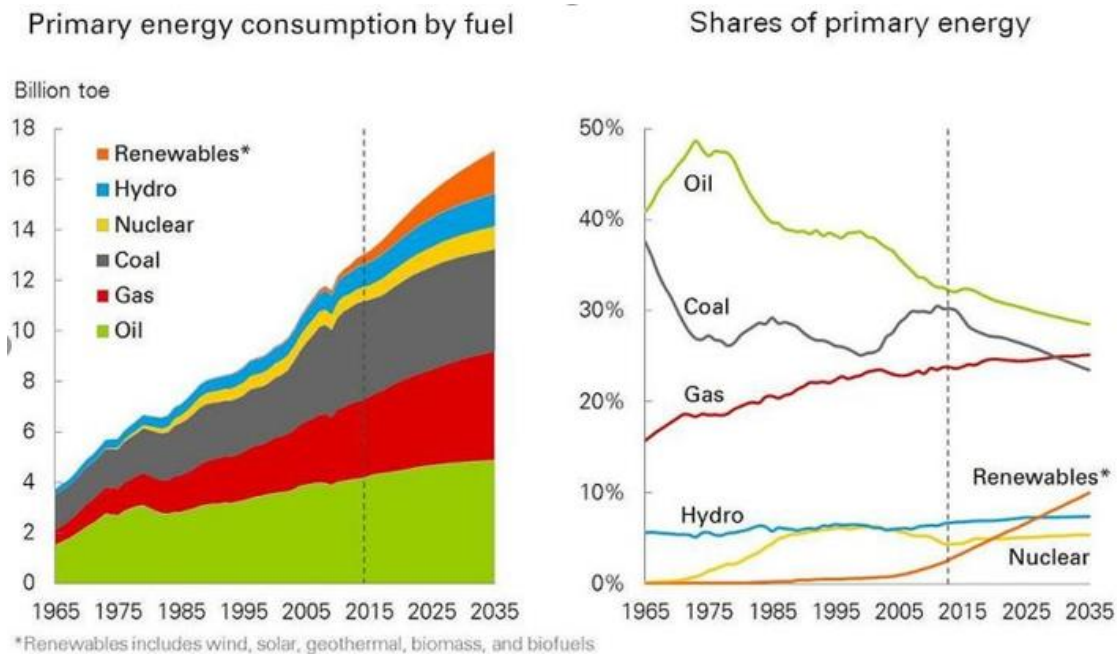
Fig 1. Primary energy consumption by fuel from 1965 to 2035 [1]

Nevertheless, with the excessive burning of fossil fuel, another challenge that people are facing is the environmental degradation. Especially global warming that has a considerable

1

influence on our eco-environmental balance, resulting in glacier melting, sea level rise and so on. The major component leading to this phenomenon is carbon dioxide (CO_2) and fossil fuel burning contribute to 73.2% greenhouse gas emissions (Figure 2) [2], According to the figure from Our World in Data, CO_2 emission from the fossil fuels burning for energy production went up to 31.5 gigatons in 2020 [3], it was seven times more than what it was in 1950s. As a result, no matter for the development of sustainable society or the energy resource availability, the energy resources' transition from fossil fuel to renewable energy is demanding.

Fig 2. Global greenhouse gas emissions by sector [2]

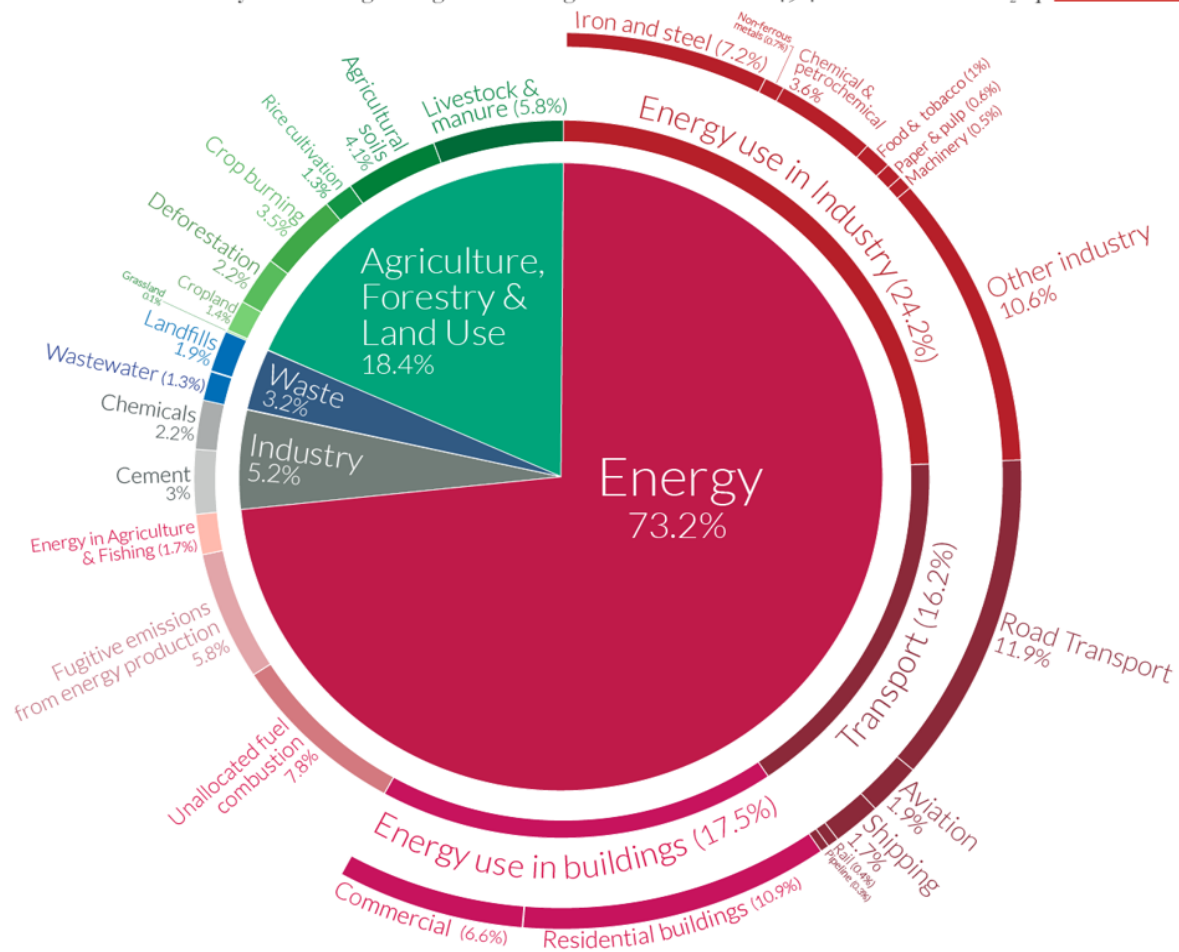Recycling CO_2 into green fuels is one of the most effective ways to alleviate the greenhouse effect and renewable energy demand. There are many approaches available for CO_2 conversion, such as electrochemical reduction, photochemical reduction, thermochemical reduction and so on [4]. Among these methods, CO_2 electro-reduction is promising and catches scientists' attention because of i) the reaction process can be controlled by adjusting the electrode potential and reaction temperature, ii) the electrolyte can be recycled, iii) the electrochemical reaction devices is very compact and easy to scale up and iv) economic feasibility.

After the electro-reduction reaction, CO_2 was reduced into value-added products, for instance, carbon monoxide and formic acid are the most likely compounds. In addition, carbon monoxide, a key feedstock, can react with hydrogen to produce hydrocarbons, meantime, CO is an industrial gas and extensively utilized for the bulk chemicals production. Formic acid is also an important ingredient for organic syntheses and already applied for textile manufacture. In recent years, it was also investigated as a fuel additive for automobiles. In fact, any carbon-based product is superior than CO_2 from perspective of environment protection, because it is stable and account for around 65% of greenhouse gas emissions (Fig 3).
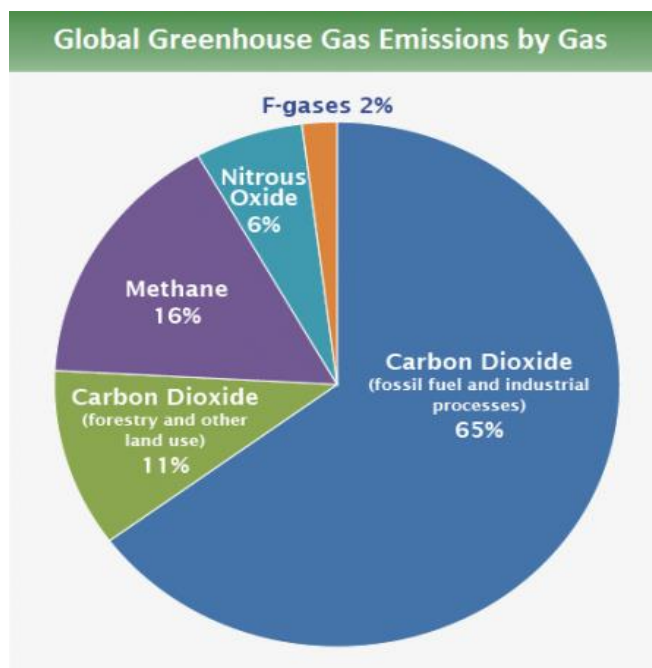
Fig 3. Global greenhouse gas emissions by gas [3]

In previous work, we synthesized CuFe LDH and NiFe LDH with different methods (such as solution aging and hydrothermal digestion, the yielded materials were dried with different methods, for instance air drying, vacuum drying and freeze drying) and used as a catalyst CO_2 electro-reduction. We found that LDH modified glassy carbon electrode (GCE) showed a positive effect on CO_2 electro-reduction where the CO_2 reduction potential was -1.6 V against the bare GCE electrode (-1.9 V). Admittedly, LDH is a semiconductor material with high chemical reactivity, however, the disadvantage of LDH is its low electrical conductivity, which can construct CO_2 reduction reaction by low electron transmission during the reaction. Besides, another bottleneck of LDH is, it possesses low specific surface area and can't adsorb much CO_2 at the same time leading to low mass transmission. In this thesis, we combined LDH with rGO to form a LDH-rGO composite and expected the unique electrical properties of rGO can overcome the drawback of the LDH and improve CO_2 electro-reduction reaction activity. Consequently, it was found that with the help of rGO, the composite showed low reduction potential and high current response.

2. Review of Literature

2.1. Layered double hydroxide

In recent year, layered double hydroxide (LDH) has attracted much attention because of its unique two-dimensional structure and wide potential applications in many areas. For instance, i) catalyst [5], ii) anion exchangers [6] and iii) adsorbing materials [7] etc. The LDH's feature is of hydrotalcite-like materials. The structure of hydrotalcite ($Mg_6Al_2(OH)_{16}CO_3 \cdot 4H_2O$) is formed by stacking positive charged $Mg(OH)_2$ layers where a proportion of Mg^{2+} is replaced by Al^{3+} and then the anion layers (CO_3^{2-})in the middle of $Mg(OH)_2$ layers to offset the positive charge (Fig 4) [8].

Layered double hydroxide (LDH) are a class of ionic solids characterized by a layered structure with the generic layer sequence $[AcB\ Z\ AcB]_n$, where c represents layers of metal cations, A and B are layers of hydroxide (OH^-) anions, and Z are layers of other anions and neutral molecules (such as water) [9]. Lateral offsets between the layers may result in longer repeating periods.

In the most studied class of LDHs, the positive layer (c) consists of divalent and trivalent cations, and can be represented by the formula:

$$[M^{2+}_{1-x}N^{3+}_x(OH^-)_2]^{x+}\ [(X^{n-})_{x/n} \cdot yH_2O]^{x-}$$
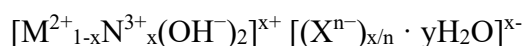
where X^{n-} is the intercalating anion (or anions).

Most commonly, $M^{2+} = Ca^{2+}$, Mg^{2+}, Mn^{2+}, Fe^{2+}, Co^{2+}, Ni^{2+}, Cu^{2+} or Zn^{2+}, and $Ni^{3+}$is another trivalent cation, possibly of the same element as M. Fixed-composition phases have been shown to exist over the range $0.2 \leq x \leq 0.33$. However, phases with variable x here also known, and in some cases, $x > 0.5$[10].

Hydroxide layer $M^{2+}_{(1-x)}M^{3+}_{x}(OH)_2$

Interlayer ● A^{n-} anions
● water molecules

○ M^{2+}/M^{3+} cations
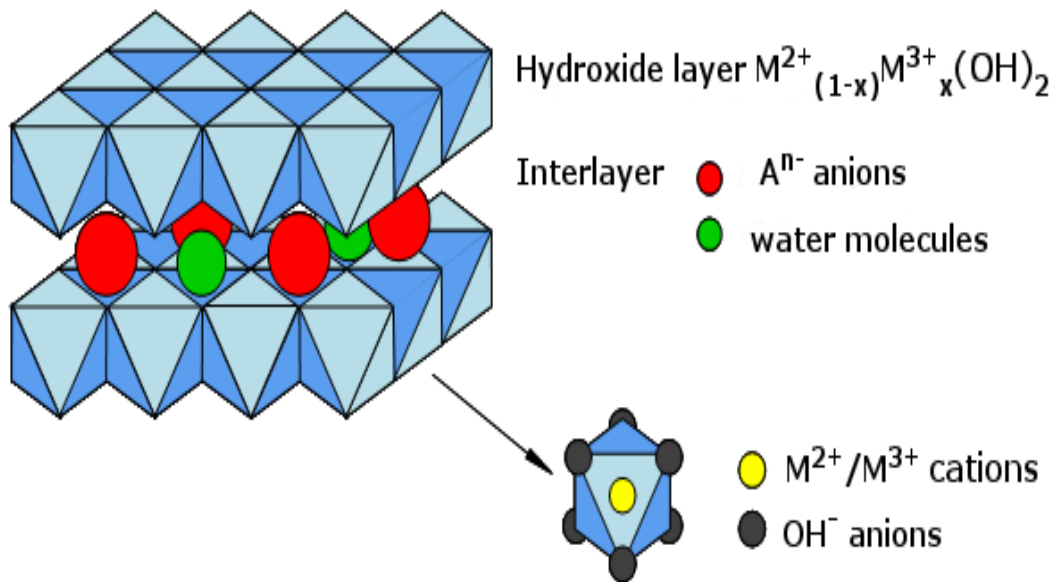● OH^- anions

Fig 4. Typical structure of layered double hydroxide [11]

By analogizing structure of brucite that has general formula $Mg(OH)_2$ we can easily gauge the structure of layered double hydroxides. The hydroxide ions in brucite is hexagonal close packing and Mg^{2+} ions are completely occupied the alternate octahedral sites, consequently, causing neutral hydroxide layers. Because of Vander Waal's attraction force, many this hydroxide layers stack one upon the other and stick together, leading to a 0.48 nm basal spacing. It can be assumed that some trivalent ions isomorphism replace a part of divalent ions in brucite lead to the mixed metal hydroxide layers with positive charge $[M_{1-x}^{2+}M_x^{3+}(OH^-)_2]^{X+}$ and the anions intercalating between the layer balance the positive charge on the mixed metal hydroxide layer, similar to layered double hydroxide structure. Besides, by hydrogen bonds, interlayer region water molecules can bind anions and the metal hydroxide layers together and enable the crystal structure of layered double hydroxide to stabilize. Because the intercalation of anions and water molecules between the metal hydroxide layers, the basal spacing increase from 0.48 nm in brucite to 0.77 nm in hydrotalcite.

There are many methods available for LDHs preparation, for instance hydrothermal methods [12], co-precipitation methods [13, 14], urea hydrolysis [15] and sol-gel methods [16, 17]. Co-precipitation is the most common method among these methods, because it can yield a high-pure and high crystallinity LDHs. In our experiment, we use co-precipitation method for LDHs preparation. Admittedly, LDHs prepared with co-precipitation method feature metal salts as metal ion precursors, alkali (NaOH) and alkali metal carbonate (Na_2CO_3) as precipitating agents.

Layered double hydroxides have prominent properties for example: unique structure, mixed metal hydroxide layers, exterior hydroxyl groups, ease of synthesis, electrochemical activity, non-toxicity, flexible anions and cations' tunability, biocompatibility, remarkable chemical and thermal stability, high surface/volume ratio, superb anion exchangeability, sustainable transmission of intercalated anions. Because of these properties, pure layered double hydroxides layered double hydroxides embedded with functional materials and layered double hydroxide nanocomposites, particularly carbon based graphene becoming the popular materials for wide applications. There are some significant applications of LDH and hybrid LDH nanocomposites were reported for instance energy storage and conversion [18], drug delivery [19], electrocatalysis [20], sensor [21] and so on. In this thesis, the LDH-rGO composite was synthesized by coprecipitation and employed as a catalyst for CO2 electro-reduction.

2.2 Graphene

In 2014, the freestanding form of graphene was isolated, thereafter, graphene based materials research grown significantly, because of its' unique thermal, electrical and mechanical properties. Further it has a large specific surface area, approximately 2630 m^2 g^{-1} [22], low band gap, high electrical conductivity, approximately 10^6 S/cm [23], and thermal conductivity between 3000–5000 W/m/K [24], high Young's modulus around 1.0 TPa [25], high tensile strength (130 GPa) [26], and widely applicable electro-catalytic

activity, these characteristics indicate that graphene is an ideal material for utilizing in electrochemical applications.

Graphene, a single layer of atoms arranged in a two-dimensional honeycomb lattice of sp^2 hybridization of carbon atoms, as shown in Fig 5 [25]. It can be wrapped into zero-dimensional balls and rolled into one dimensional single or multi-walled carbon nanotubes which depends on the number of graphene layers. In addition, more than 10 layers of graphene stacking together can form graphite. Therefore, graphene can be considered as the foundation of all carbon forms. The graphene can be oxidized into graphene oxide (GO) by oxidizing agent or spontaneously contacting with air, that is another form of graphene. But graphene oxide should be reduced in electrochemical or other chemical methods before use.
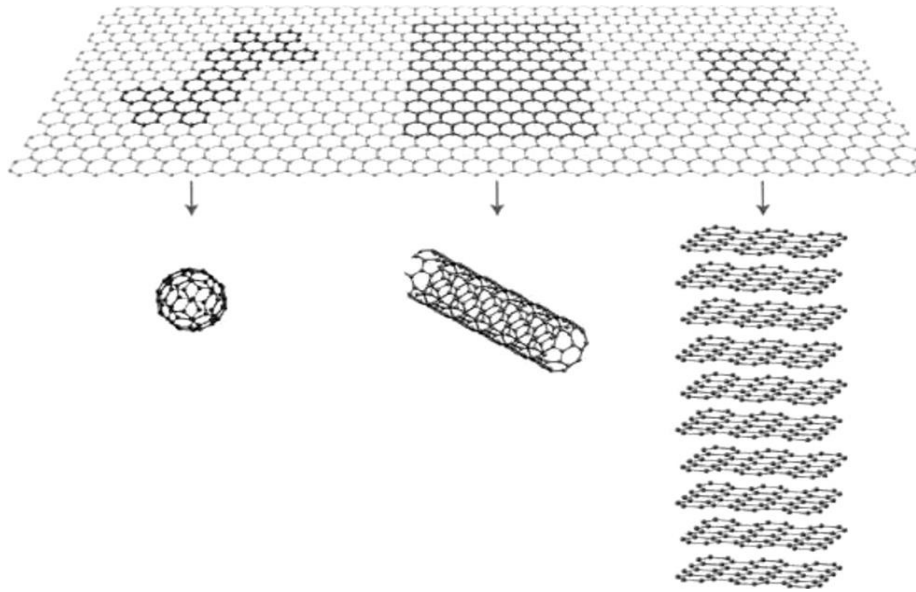
Fig. 5. Schematic representation of graphene, which is the foundation material for other carbon forms, such as fullerene materials, buckyballs, carbon nanotubes, and graphite [25].

In general, there are two synthetic methods for graphene preparation, top down method and bottom up method, based on the classification of synthesis methods for materials as shown in Figure 6. Top down methods are a collection of exfoliation approaches, such as

mechanical exfoliation and chemical exfoliation. It begin with the bulk materials and by breaking the week bond with mechanical method, chemical method or other forms of energy and separating graphite into a single layer of graphene sheet. On the contrary, bottom up methods start from small species, such as atom or molecule, to grow the target materials in size by chemical reaction. It includes pyrolysis, epitaxial growth, thermal and plasma-enhanced chemical vapor deposition (CVD). It is worth noting that different synthesis methods defines the properties of graphene, which means there is no a single approach of graphene preparation that yields graphene presenting high performance for all potential applications [23].
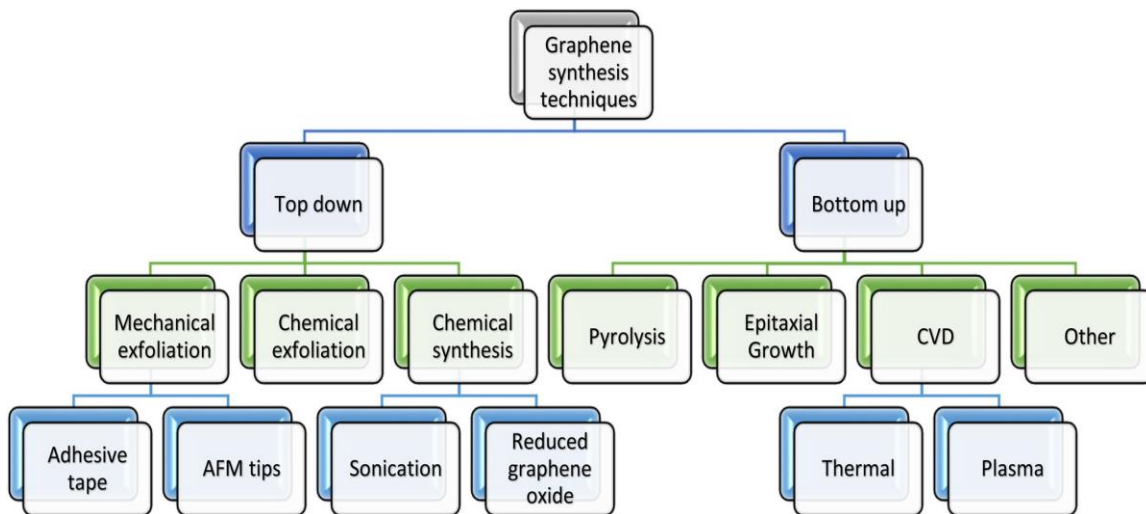
Fig 6. Graphene synthesis methods [27]

In our experiment, we utilized chemical synthesis methods to prepare reduced graphene oxide (rGO) by reducing graphene oxide (GO) (Fig 7). Graphene oxide is one kind of functionalized graphene. It possess oxygen content (hydroxyl, carboxyl) on the basal carbon planes and is the most significant graphene derivatives. Due to the existence of oxygen-containing groups, the chemical reactivity and solubility of graphene are both enhanced. Because of its low cost and high chemical reactivity, graphene oxide has been extensively employed in many industries, for instance, it was considered to be a promising material for water remediation [28][29], and can be employed in fuel cells for sustainable

energy production [30][31], as drug delivery [32][33] and catalyst [34] and so on. GO was prepared with modified hummers methods where graphite powder was oxidized in the presence of concentrated H_2SO_4 and $KMnO_4$. After reduction, almost all oxygen-containing chemical groups were removed and reduced graphene oxide (rGO) was obtained.

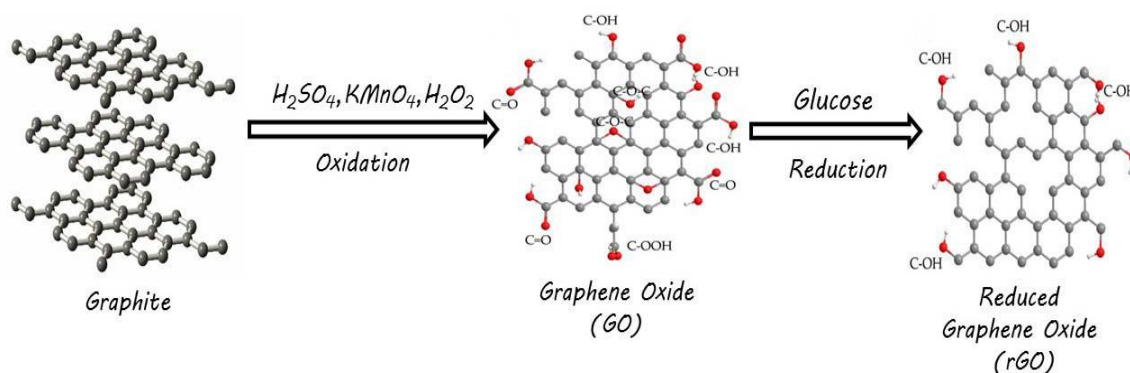Fig 7. Mechanism of synthesis of GO and rGO [35]

Graphene possesses exceptionally good thermal, electrical and mechanical properties, For instance, it has a large specific surface area that is crucial characteristic of an electrode material, especially in energy storage, approximately 2630 m^2/g, whereas the specific surface area of single-walled carbon nanotubes and graphite are $\sim$1315m^2 g^{-1} and $\sim$10m^2 g^{-1} respectively [7]. Besides, due to the extensive conjugated sp^2 carbon network, the electrical conductivity of graphene can reach to 64mS cm^{-1}; it is almost 60 times more than the electrical conductivity of single-walled carbon nanotubes. What's more interesting is that, it can be stable in a wide range of temperatures, which is quite important for the reliability of energy-associated applications. In addition, graphene shows the half-integer quantum Hall effect even at normal temperature, and its Fermi velocity is approximately 10^6m s^{-1}, which means graphene possesses exceptional electronic quality.

Thus the utilization of graphene in future applications to aid with technological advances within energy related fields holds great promise, where the years of research based upon various other carbon forms can be readily tailored to graphene.

In terms of application, the two-dimensional graphene was more remarkable than other forms of carbon atoms in twenty-first century. It was predicted that graphene will be at the center of future prospects and the application of graphene is promising for technology advancements in energy storage and conversion areas. Graphene is an ideal material and can be widely utilized in numerous applications. Such as graphene effect transistors [36], supercapacitors [37], graphene-based anode for lithium battery [38][39], biosensor [40] and so on. Yawei Li et al. [41] investigated graphene supported transition metal dimers (Cu, CuMn, CuNi) as a catalyst on CO_2 electroreduction and found a better performance with low reduced overpotential and enhanced current density. Phan and colleagues [42] also found graphene supported Cu nano-cuboids where Cu showed long-term stability, high product selectivity on CO_2 electro-reduction. In this work we combine graphene with LDH to form a composite and expect the superb properties of graphene could improve the electro-conductivity and catalytic activity of the composite.

2.3 CO_2 electro-reduction reaction

CO_2 recycling is a potential promising method to reduce the content of CO_2 in the atmosphere and alleviate greenhouse effect. It has been broadly researched since nineteen century and metal electrodes were of particular interest. In 1985, Frese and co-workers found that ruthenium electrode presented a considerably catalytic activity on CO_2 electro-reduction. In CO_2 electro-reduction process, a potential difference was applied between cathode and anode and CO_2 was reduced on the surface of cathode.

Fully oxidized carbon dioxide is a unpolarized and linear-shaped molecule, it is chemically inert and quite stable where the gap between the low un-occupied molecular orbital (LOMO) and highest occupied molecular orbital (HOMO) is too large, approximately 13.7 eV and the potential applied for CO_2 - one electron reduction is over 1.9 eV. The most common electrolyte for CO_2 electro-reduction is water, but the problem is the solubility of CO_2 in water, which is poor at acidic and neutral condition. So the reduction of carbon

dioxide is kinetically sluggish process and an highly efficient catalyst is needed for developing this reaction. In order to accelerate CO_2 electro-reduction reaction, homogeneous and heterogeneous catalysts is employed and it truly improves the reaction, for example, homogeneous catalyst can develop the selectivity. But the drawback is some of homogeneous catalysts are noxious, instable, high cost and hard for post-separation. But for carbon-based materials, metal and metal oxide like heterogeneous catalysts the drawbacks are less.

The researchers have studied the principle of electrochemical carbon dioxide reduction for decades to clarify the relationship between different kinds of catalysts and products of the reaction. Finally on the basis of the understanding of electrochemical carbon dioxide reduction (ECR) on metallic electrodes, researchers propose new reaction pathways of ECR.

Generally speaking, depending on the different catalysts and reaction conditions. There are four possibility of reaction pathways involved in electrochemical reduction of carbon dioxide, to be more specific, reaction pathway of two electrons, four electrons, six electrons and eight electrons [43], which take place in the electric double layer, in other words, the interface of electrolyte-electrode. Normally, the catalyst stick on the electrode and CO_2 reach to a saturation state in the electrolyte. Usually there are three steps in catalytic procedure:

1. Carbon dioxide was adsorbed on the catalyst.

2. Electron transfer and/or proton migration in order to break C–O bonds and/or C–H bonds emerge.

3. As a result, reconfiguration and the product was desorbed from the surface of catalyst and migrate into the electrolyte [44].

The kind of electrocatalyst used and the potential imposed on the electrode has a big impact

on the final products. Generally, the final reduction products are a mixed carbon compounds with diverse valence states. Including formic acid, carbon monoxide, methanol, formate, ethanol, methane, ethylene and so on [45,46]. Electrochemical carbon dioxide reduction is a surface phenomenon, Therefore, there is no general reaction route to the target products. In reality, the morphology, type and nature of the catalyst play a big role in the reaction mechanism, besides, number of shifted electrons, the selectivity of the electrocatalyst to the specific intermediate, energy barrier needed for electron transfer also influence the reaction mechanism. Figure 8 display the energy barrier for different number of electrons transferred.

$CO_2 + 2H^+ + 2e^- \rightarrow CO + H_2O$	$E^0 = -0.53$ V
$CO_2 + 2H^+ + 2e^- \rightarrow HCOOH$	$E^0 = -0.61$ V
$CO_2 + 4H^+ + 4e^- \rightarrow HCHO + H_2O$	$E^0 = -0.48$ V
$CO_2 + 6H^+ + 6e^- \rightarrow CH_3OH + H_2O$	$E^0 = -0.38$ V
$CO_2 + 8H^+ + 8e^- \rightarrow CH_4 + 2H_2O$	$E^0 = -0.24$ V
$CO_2 + e^- \rightarrow CO_2^-$	$E^0 = -1.90$ V

Fig 8. Summary of thermodynamic potentials of CO_2 reduction to various products. [47]

The CO_2 recycling was based on the formation of nuclei and chemical bonds. As mentioned earlier, for carbon dioxide electrocatalysis, there are three steps. Firstly, carbon dioxide receive one electron and from an essential intermediate $CO_2^{\bullet-}$, which is the most challenging step and the major reaction rate limiting step, involving reconfiguration from linear molecules to bending radical. Sufficient energy is needed to overcome the barrier, in order for this kinetically slow reaction to proceed at a satisfactory rate, an overpotential of -1.9 V vs. reversible hydrogen electrode (RHE) is required. Secondly, the active $CO_2^{\bullet-}$ take thermodynamically favorable and instantaneous proton-coupled multiple-electron-transfer

reactions. The last step is rearrangement of product species.

Wan et al [48] summed up the Science Citation Index-listed periodicals and showed there were total 855 papers related to molecular-based catalysts published in academic journals from 1999 to 2009. Most of metal and metal oxide was employed as a catalyst for electro-reduction of CO_2. Among them, some of metal and metal based materials showed profound result on CO_2 electro-reduction. For example, Lehn et al. [49] studied the Rhenium-based materials $Re_{(I)}(bpy)(CO)_3Cl$ on the electrochemical reduction of CO_2 to CO and found the CO_2 reduction potential was dramatically deduced, approximately -1.25 V against the bare Glassy carbon electrode (GCE). Iron-based materials also presented an higher reactivity toward CO_2 conversion. Gu et al. [50] revealed that the CO_2 started to reduce at low overpotential (80 mV) in 0.5 M $KHCO_3$ solution with the iron-based catalyst, single-atom $Fe(III)X_4$ where X can be C and N. In addition, Carbon nanotube supported catalysts presented high performance on CO_2 electro-reduction than metal-based electrodes or metal-based catalysts, such as carbon nanotubes supported iron nanoparticles presented high catalytic activity on CO_2 electro-reduction to form C_2H_4 [51]. Chen and coworkers [52] employed Au nanoparticles as a electrocatalyst on electrochemical reduction of CO_2 to CO, a high selectivity and a low reduction potential (140 mV) was observed. Besides the metals and metal composites, organic molecules can also be investigated as a catalyst on CO_2 electro-reduction. Aydin et al. [53] employed polypyrrole (PPy) as an electrode for CO_2 reduction and a low reduction potential, approximately 0.4 V was observed. Aromatic amine catalysts [54], Enzyme catalysts [55] also showed high performance on CO_2 electroreduction.

Although there are some advancement in CO_2 electro-reduction after years of development, there are still some challenges: i) larger overpotential between LOMO and HOMO, ii) low exchange current densities, iii) low products selectivity, iv) nondurable electrodes. Consequently, a low-cost, robust catalyst that can enhance the CO_2 electro-reduction reaction at satisfactory rate is the focus in the further research.

2.4. Objectives of the work

This work consists of synthesis, characterization and application of layered double hydroxide-reduced graphene oxide composite for CO_2 electroreduction. Recently, some papers have stated that metal and metal based LDH is beneficial for the improvement of CO_2 reduction activity [56]-[60]. In our previous work, nickel ferrous layered double hydroxide and copper ferrous layered double hydroxide were prepared and employed as a catalyst in CO_2 electro-reduction. It was proved that the LDH showed a considerable catalytic activity on CO_2 reduction, the reduction potential was -1.6 V against bare electrode -1.9 V. However, low electrochemical conductivity, the intrinsic shortage of LDH, limit its activity. So the catalytic effect of LDH-based composite with the presence of rGO was investigated during the CO_2 electro-reduction process, by comparing the LDH-$rGO_{1,2,3,4}$ composites where $rGO_{1,2,3,4}$ were prepared with different reduction methods in different reaction conditions with pure LDH. With the presence of rGO, the catalytic activity of LDH-based composite might show a low overpotential on CO_2 reduction. This was the ideological basis of our work.

3 Experimental

3.1 Chemicals and Materials

$Ni(NO_3)_2.6H_2O$, $Fe(NO_3)_3.9H_2O$, ammonia-NH_3, NaOH were purchased from Sigma-Aldrich and used as received. Na_2CO_3 was purchased from FF chemicals. Graphite, $KMnO_4$, H_2SO_4, H_2O_2, HCl, $NaBH_4$. VERTEX 70 FT-IR Spectrometer, Ultrasonic cleaner USC-THD (VWR), Autolab (Metrohm).

0.1 M aqueous solutions of $Fe(NO_3)_3.9H_2O$, $Ni(NO_3)_2.6H_2O$ were prepared. 2 M aqueous solutions of NaOH and Na_2CO_3 were prepared. All solutions were prepared with DI (Deionized) water.

3.2 Synthesis of Nickle ferrous layered double hydroxide (NiFe LDH) – Co-precipitation

The synthesis procedure was presented in Figure 9. 0.1 M aqueous solution of metal salts 1) Nickle (II) nitrate hexahydrate $Ni(NO_3)_2.6H_2O$, and 2) Iron (III) nitrate nonahydrate $Fe(NO_3)_3.9H_2O$ (with a ratio of 3:1) were added in 500 mL of DI water. The theoretical amount of Ni :Fe = 5.7239 : 2.4531 mmol aiming for 1000 mg of product LDH material. 2 M solution of NaOH (16.354 mmol) and 2 M solution of Na_2CO_3 (12.2655 mmol) were added dropwise from two different burette to the above metal solution mixture, at a rate of 1 mL.min^{-1}. The theoretical ratio of NaOH : Na_2CO_3 = 13.33 : 1. The pH of the coprecipitation medium was measured to be 9-11. Meanwhile, sodium carbonate (2M) solution was added into the flask in order to form $CuFeCO_3$ complex. The synthesis of LDH was carried at room temperature and under steady stirring, aiming for the homogeneity of the reaction. The reaction solution was maintained for 2 h until the final slurry was generated. After the formation of LDH precipitate, the mixture was stirred for half an hour to enhance the formation of LDH [8]. Next, the LDH materials were washed

and centrifuged several times until the PH value =7, so as to remove the impurities. Eventually, the co-precipitation material was dried by freeze dryer at -80 °C for 16h.
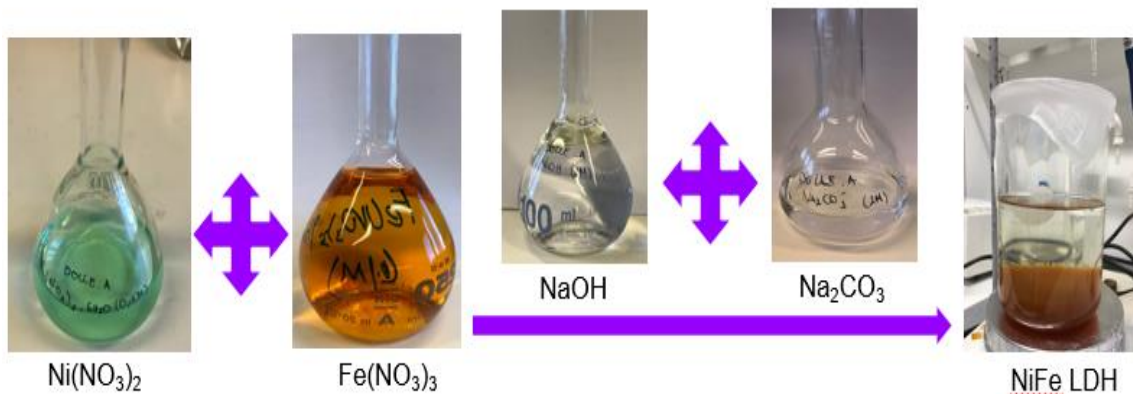

Fig 9. Schematic representation of NiFe LDH preparation

3.3. Synthesis of Nickle ferrous layered double oxide (NiFe LDO) – Calcination

Besides LDH, in this work, we also prepared Layered double oxides (LDOs) by heat treatment. NiFe LDO was prepared by calcination method by directly calcining NiFe LDH in the air at 500 ℃ and maintaining the reaction for 4 h and let it cool down by itself.
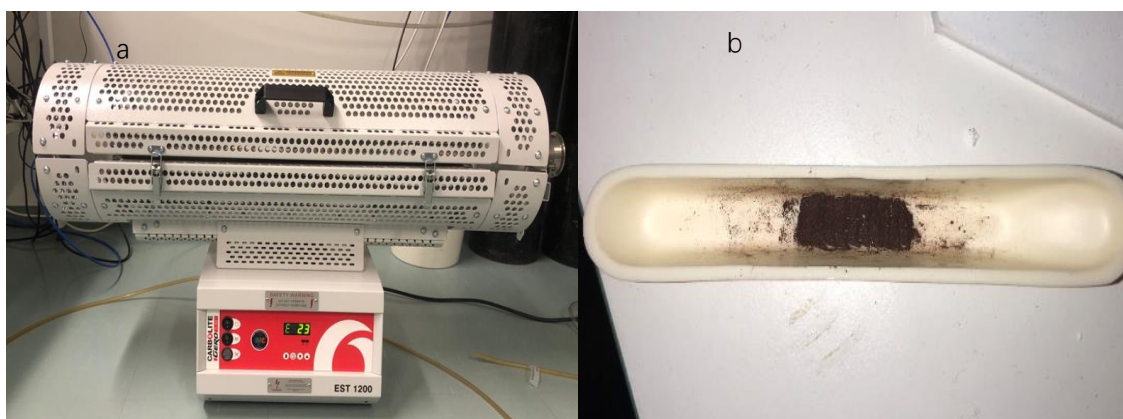

Fig 10. (a)Tube furnace (b) NiFe LDO.

3.4. Synthesis of graphene oxide (GO) – modified hummers method

Graphene oxide was prepared using modified hummers method (Figure 11). 96 ml concentrated H_2SO_4 and 1 gram of $NaNO_3$ was added in a round flake. Then, 2 grams of graphite flakes were added into the solution. 6 grams of $KMnO_4$ was slowly added to the solution in half an hour. Because it's an oxidation process and will release a lot of heat, so the reaction took place in the condition of ice water bath. Then the solution cooled down for 2 h in the ice water bath. Further the solution was taken out from ice water bath and left it at 35 °C for 5 days. Next step was adding 240 ml deionized water in the reaction solution and stirring the solution overnight. And then 50ml 30% H_2O_2 was added into the solution to remove unreacted $KMnO_4$, you can see clearly the color of reaction solution turns from brown to yellow. Centrifuging the solution and washing the graphite oxide several times until pH value equal to 7. The washed graphene oxide solution was dried in vacuum oven to yield the powder of GO. Finally, the GO solution was synthesized by dispersing GO powder in deionized water with the concentration of 5 mg/ml.
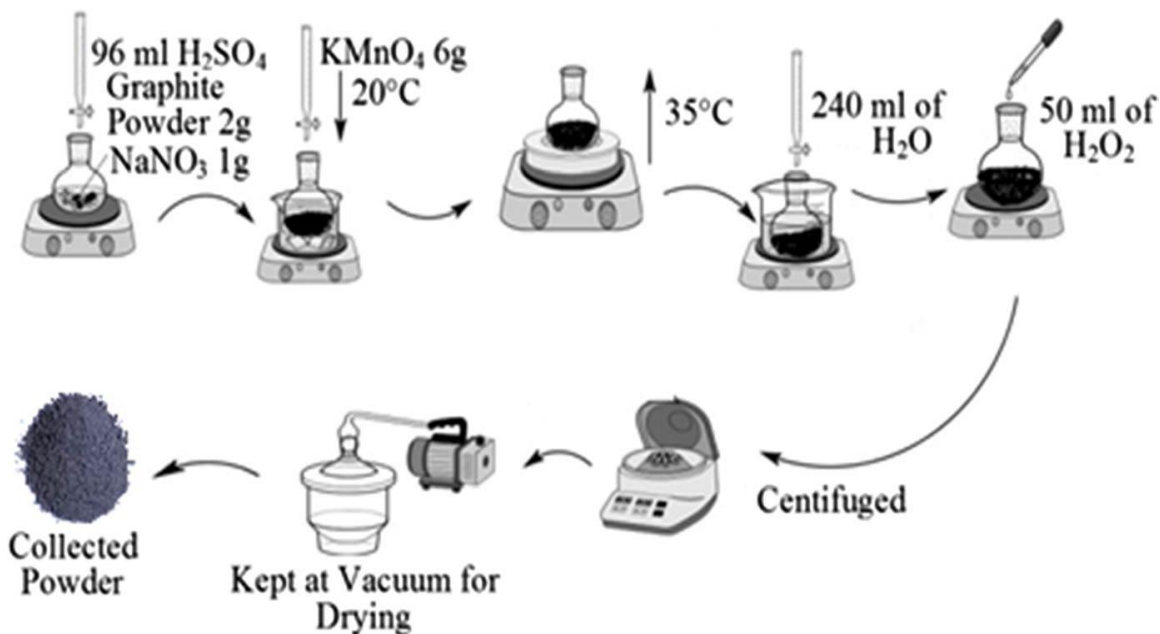

Fig. 11. Schematic representation of graphene oxide synthesis with modified Hummer method.[61]

3.5 Synthesis of reduced graphene oxide (rGO) – Chemical reduction

In this thesis, chemical reduction methods were used for the preparation of reduced graphene oxide. The GO was reduced by i) hot water and ii) NaBH$_4$ in both neutral and alkaline condition.

3.5.1 Hot water reduced GO – neutral condition

3ml of 5mg/ml GO solution was added in a three-necked flask with 200 ml deionized water. It was kept stirring to disperse GO evenly and the reaction solution was heated at 98 °C in oil with water flux for 2h until the color of the solution turned from brown to dark. After that, the flask was removed from oil bath and allowed to cool down for half an hour at room temperature. Then the rGO solution was washed and centrifuged several times. The following step was to dry the centrifuged material in the air at 110°C overnight to produce dried rGO$_1$.
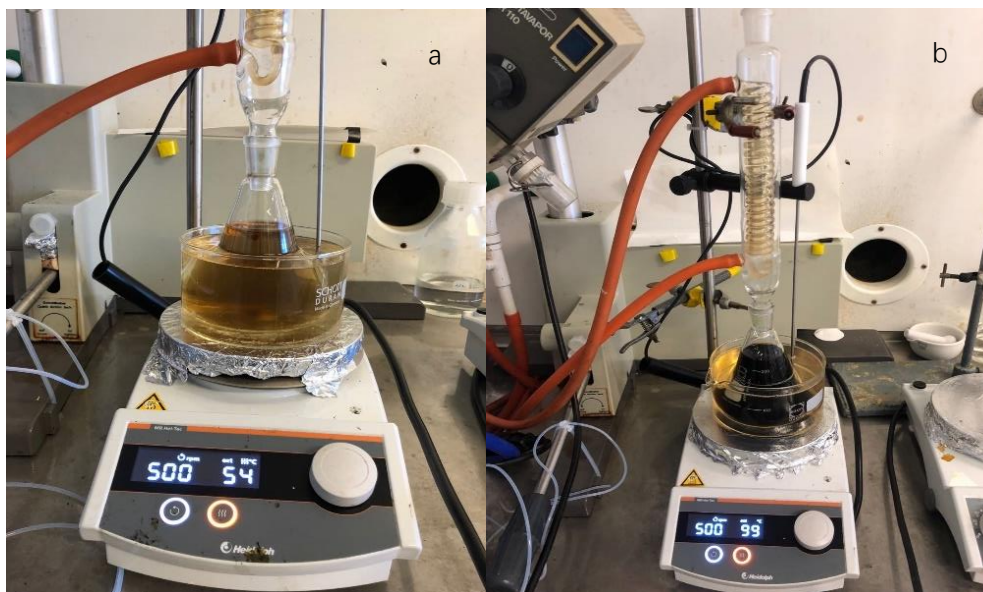
Fig 12. (a) GO and (b) rGO solution.

3.5.2 Hot water reduced GO – alkaline condition

3ml of 5mg/ml GO solution was added in a three-necked flask with 200 ml deionized water, 6-8 drips of ammonia was added in the solution to create an alkaline condition (pH = 10), the reason for adding ammonia was because the reduced graphene oxide possessed less oxygen content leading to decrease in surface potential, as a result, the dispersion of rGO in solution got stacked tightly and was easy to form irreversible aggregation. By adding ammonia to alter pH value and increase the negative surface charge of rGO the aggregation was prevented. To disperse GO evenly the solution was under constant stirring and then heated at 98 °C in oil with water flux for 2 h until the color of the solution turned dark from brown. After that, the flask was removed from oil bath and allowed to cool down for half an hour at room temperature. Then the rGO solution was washed and centrifuged several times. The following step was to dry the centrifuged material in the air at 110 °C overnight to produce dried rGO_2.

3.5.3 NaBH₄ reduced GO – neutral condition

3ml of 5mg/ml GO solution and 600 mg $NaBH_4$ ($GO:NaBH_4$=1:4) were dispersed in 200 ml DI water in a conical flask, the reaction solution was stirred at room temperature for 2h until the color of the solution turns from brown to dark. After that, the rGO solution was washed with deionized water, centrifuged several times until pH =7 and then dried in the air at 110 °C for 16 h to yield dried rGO_3.
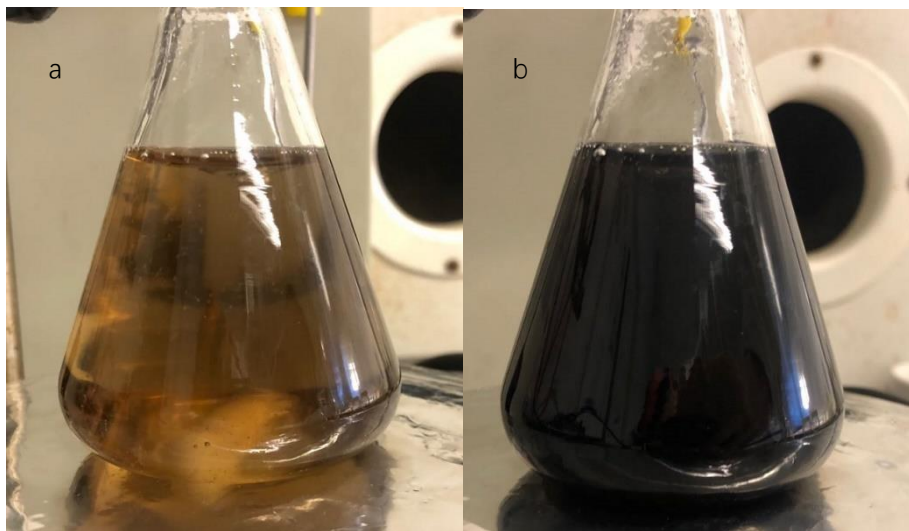
Fig 13. (a) GO solution and (b) rGO solution reduced by NaBH₄.

3.5.4. NaBH₄ reduced GO – alkaline condition

3ml of 5mg/ml GO solution and 600 mg NaBH₄ (GO:NaBH₄=1:4) were dispersed in 200 ml DI water in a conical flask, in order to prevent the aggregation of rGO, 3-5 drops of ammonia was added into the solution to create a alkaline condition (pH = 10), the reaction solution was stirred at room temperature for 2h until the color of the solution turns from brown to dark. After that, the rGO solution was washed with deionized water, centrifuged several times until pH =7. Then the material was dried in the air at 110°C for 16h to yield dried rGO₃.

3.6. Synthesis of NiFe LDH-rGO Composites – hydrothermal treatment

Hydrothermal method was utilized for the composite preparation. 3 mg rGO in 1 mL deionized water was sonicated for 15 minutes to break the rGO flakes and disperse evenly in water. Then the sonicated rGO solution was mixed with 3mg NiFe LDH in Teflon beaker. Then the beaker was placed in the autoclave and sealed tightly. Next, the autoclave was put and heated at 145 °C inside of air dryer for 16 h to create a higher pressure than ambient atmosphere. Then the rGO and LDH would react actively to form the composite. Finally,

the as-synthesized composite was dried in air at 110 °C for 16h. Because of 4 different types of rGO, as a result, 4 kinds of NiFe LDH-rGO composites were obtained.

Fig 14. (a) Teflon beaker and (b) stainless autoclave.

3.7. Catalyst ink preparation

The catalyst ink for electro-reduction of CO_2 was prepared with sonication method. First, 1 mg of LDH-rGO composite and 1 ml ethanol were mixed and sonicated with Ultrasonic cleaner USC-THD (VWR) for 15 minutes to break the composite flake into small particles and disperse evenly in ethanol. After that, 30 µl (6 µl each time, 5 times) catalyst ink was coated on the surface of glassy carbon electrode (GCE) by drop casting and then left it to dry. Finally a thin catalyst film was formed on the surface of GCE.

Fig 15. (a) ultrasonic cleaner and (b) catalyst ink casting.

3.8. Electrochemical measurement – cyclic voltammetry

The measurement of CO_2 electro-reduction reaction was performed with cyclic voltammetry method in a three electrodes cell system. As shown in Figure 16 a, where GCE was working electrode and the catalyst was casted on its' surface, platinum wire was counter electrode, along with Ag/AgCl worked as reference electrode. The electrolyte used for this experiment was 0.1 M Tetrabutylammonium hexafluorophosphate (TBAPF6) and dissolved in acetonitrile solvent (Fig 16 b). In the measurement, the start potential and stop potential applied on the working electrode were both -0.010 V, upper vertex potential and lower vertex potential were 0.000 V and -2.000 V respectively, the scan rate was 0.05 V/s. Firstly, N_2 gas was bubbled into the electrolyte solution with a constant flow for 15 minutes and then current was measured against applied potential at N_2 atmosphere as the background. Because N_2 was an inert gas and in this experiment the potential applied on working electrode was not sufficient to reduce N_2. Therefore, the cyclic voltammogram

should show very low current response in the presence of N_2. Then we saturated electrolyte solution with CO_2 with a constant flow for 15 minutes and measured the current against applied potential. By comparing cyclic voltammogram at CO_2 atmosphere with the background (N_2 atmosphere) CO_2 reduction potential was identified.
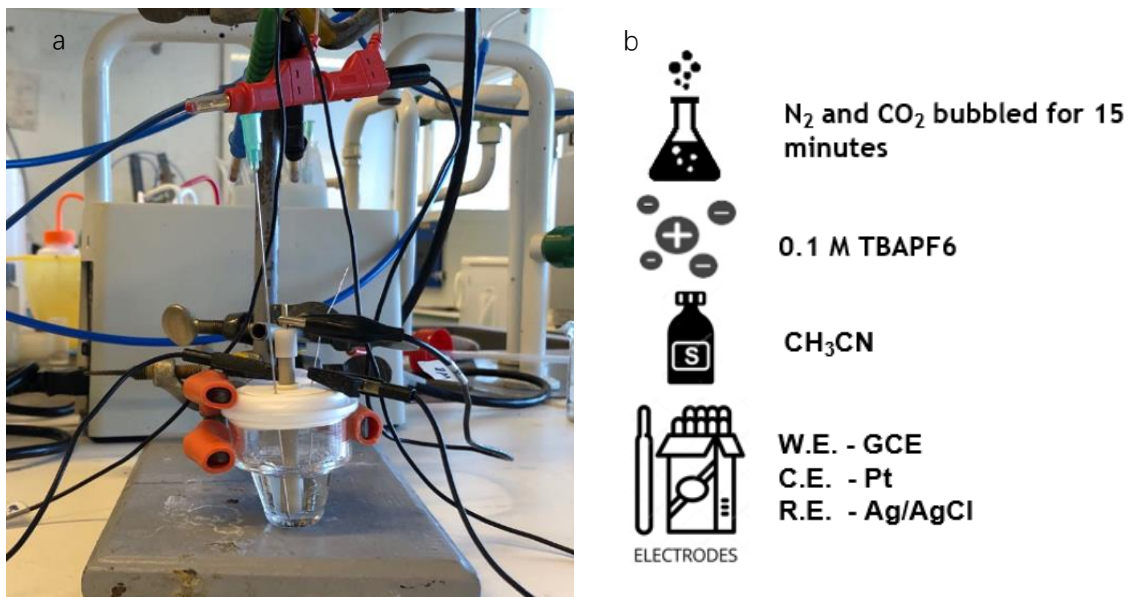

Fig 16. (a) three electrode cell and (b) the electrolyte, solvent and electrodes for electrochemical measurement.

4. Results and discussions

4.1. Characterization – X-ray fluorescence (XRF)

In this thesis, XRF was used for analysing the element composition and composition ratio of the LDH materials. As showed in Figure 17(a) the composition ratio between Ni element and Fe element was around 1.767:1, which was lower than the expected ratio 2.333:1. The XRF spectroscopy of NiFe LDH was showed in Figure.17(b) $(Fe)K\alpha_{1,2}$, $(Fe)L\alpha_{1,3}$, $(Ni)K\alpha_{1,2}$, and $(Ni)L\alpha_{1,2}$ emission were observed at 6.409KeV, 6.15 Kev, 8.51 KeV and 7.48 KeV respectively.
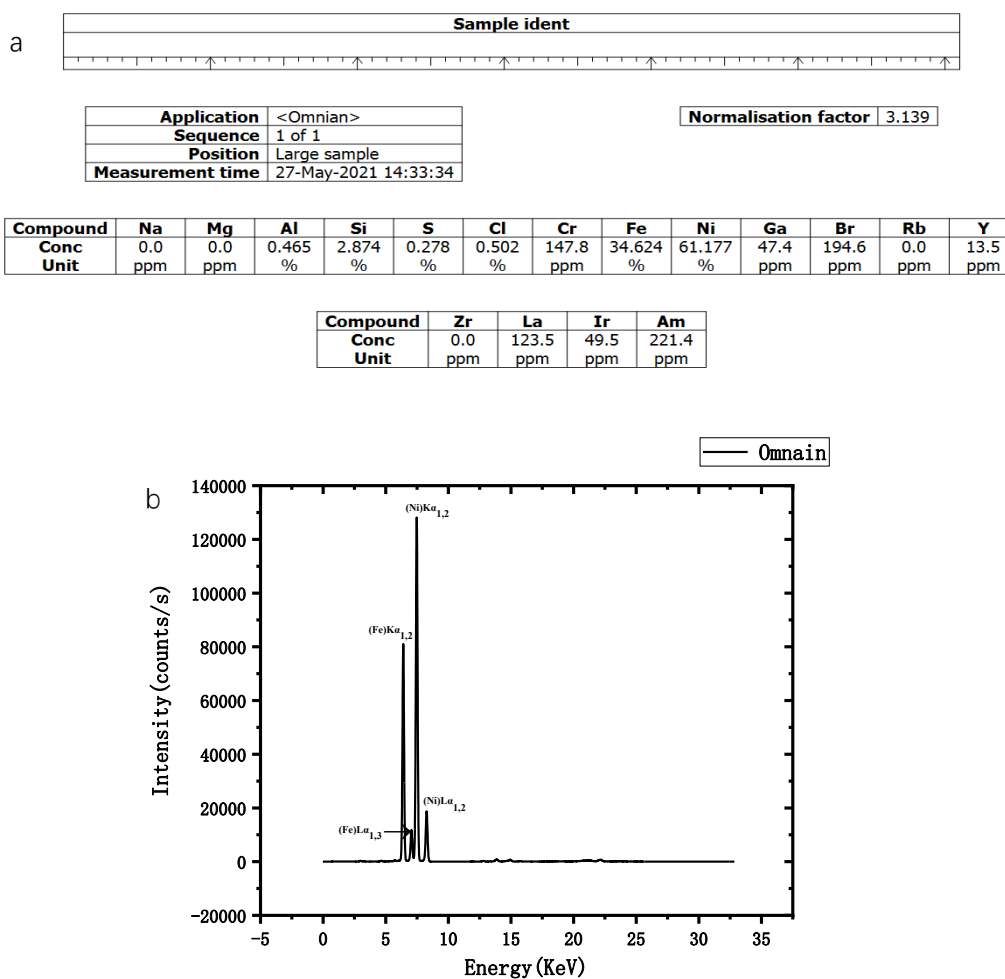
a

Sample ident

Application	<Omnian>	Normalisation factor	3.139
Sequence	1 of 1		
Position	Large sample		
Measurement time	27-May-2021 14:33:34		

Compound	Na	Mg	Al	Si	S	Cl	Cr	Fe	Ni	Ga	Br	Rb	Y
Conc	0.0	0.0	0.465	2.874	0.278	0.502	147.8	34.624	61.177	47.4	194.6	0.0	13.5
Unit	ppm	ppm	%	%	%	%	ppm	%	%	ppm	ppm	ppm	ppm

Compound	Zr	La	Ir	Am
Conc	0.0	123.5	49.5	221.4
Unit	ppm	ppm	ppm	ppm

Fig 17. (a) composition ratio of NiFe LDH, (b) XRF spectroscopy of NiFe LDH.

25

4.2. Characterization - Fourier-transform infrared spectroscopy (FT-IR)

FT-IR was an advanced technique used to characterize chemical functional groups in the materials. FT-IR spectra of GO, rGO_1 (prepared by hot water without ammonia) and rGO_2 (prepared by hot water with ammonia) are shown in Figure 18.
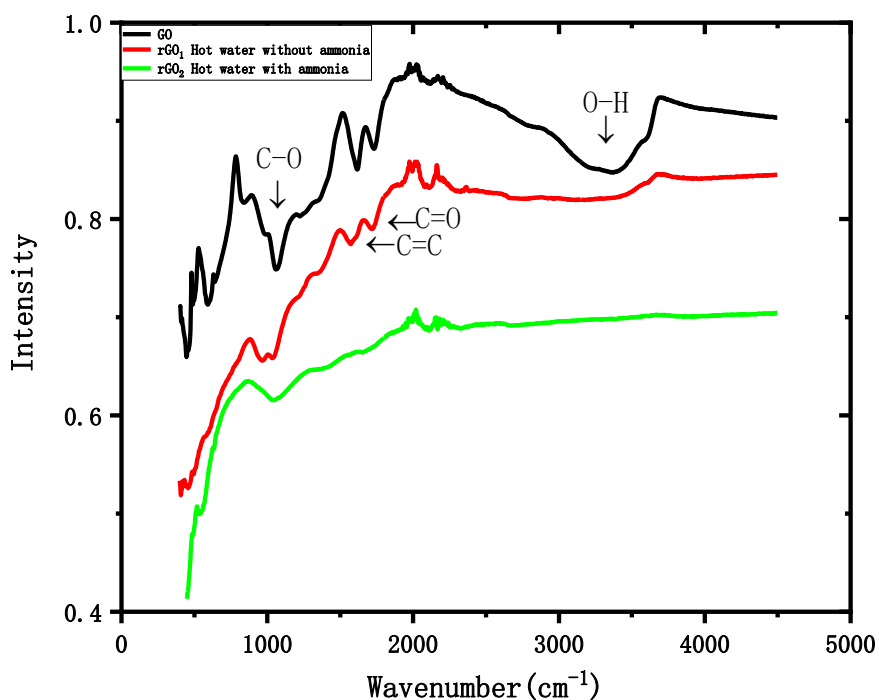

Fig 18. FT-IR spectra of GO, rGO_1 and rGO_2.

As the results stated that there were C-O, C=C, C=O and O-H chemical functional groups in GO spectra. As marked, the broad peak between 3100 cm^{-1} to 3700 cm^{-1} was corresponding to O-H functional groups. The band at 1620cm^{-1} represented C=C functional groups, and the adjacent peak at 1720cm^{-1} was corresponding to C=O oxygen-containing groups. Then the band at approximately 1055 cm^{-1} represented C-O functional groups. But after hot water treatment, there were dramatic changes in rGO_2 structure and some of those functional groups mentioned above were removed especially oxygen content, which can be assumed that the GO was successfully reduced by hot water in alkaline condition. For

example, the O-H broad peak between $3100cm^{-1}$ to 3700 $cm^{-1}$and C=O peak were disappeared completely. However, for rGO_1 prepared by hot water in neutral condition, the spectra showed that C=O and C-O groups were still in the materials, but the peaks presented having less intensity than the peaks in GO materials.

As we mentioned above, the spectra of rGO_1 reduced by hot water in neutral condition indicated that it was not reduced completely, because there were still some C=O and C-O groups left on the rGO_1 samples. Then we did some improvements by prolonging the reaction time from 2 h to 20 h and the yielded materials were characterized by FTIR again, as shown in Figure 19 .rGO_1 with 20 h reduction reaction showed the disappearance of oxygen containing groups.
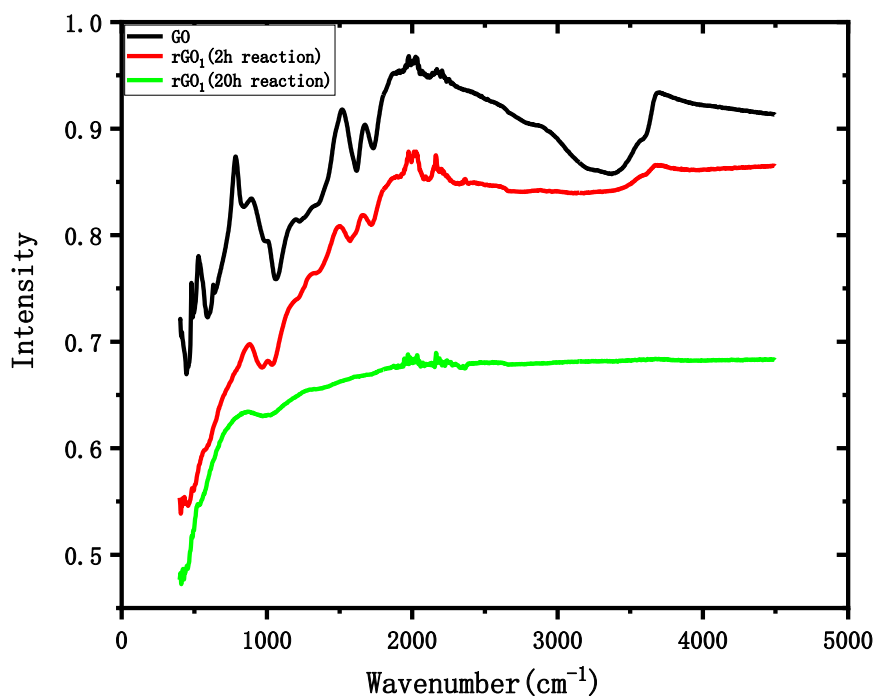

Fig 19. FT-IR spectra of GO, rGO_1 (2 h reaction) and rGO_1 (20 h reaction).

By comparing samples of rGO_1 (2 h reaction) and rGO_1 (20 h reaction) we can conclude reaction time can affect the reduction effect, along with the increase of reaction time, the reduction effect get better. The C=O, O-H functional groups were totally removed after 20 h reduction reaction, and C-O peaks at 1055 cm^{-1} showed low intensity.
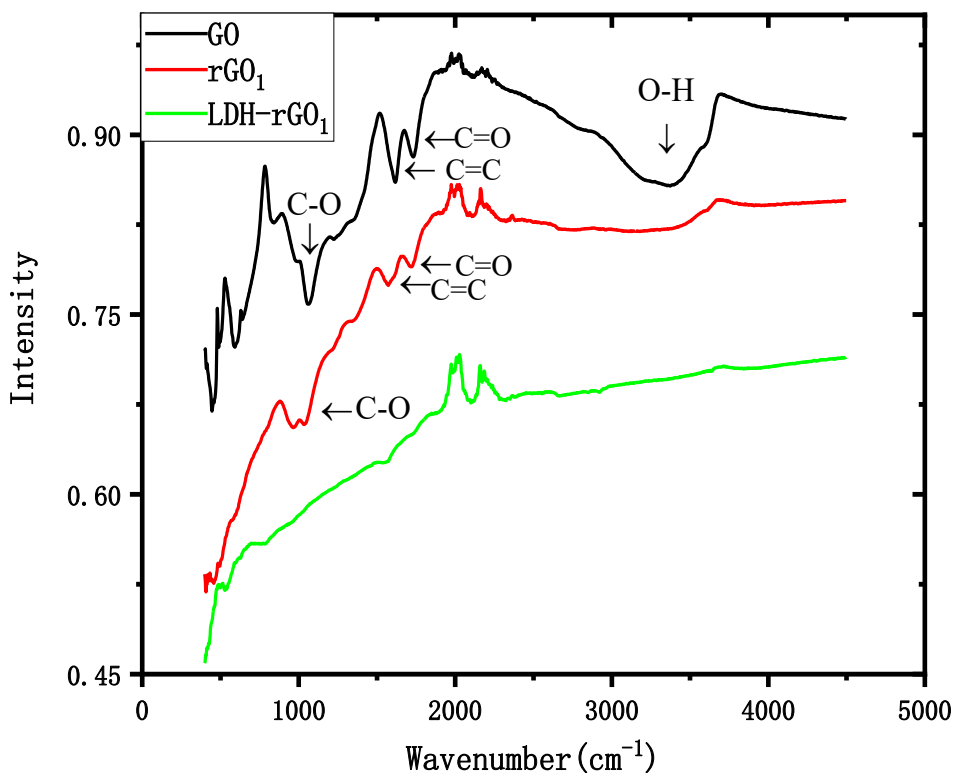

Fig 20. FT-IR spectra of GO, rGO_1 and NiFe LDH-rGO_1

FT-IR spectra of GO, rGO_1 and NiFe LDH-rGO_1 are shown in Figure 20. The red spectrum was rGO_1 (reduced by hot water in neutral condition) and it showed that there were some C=O and C-O chemical functional groups in rGO_1sheet. We can infer that the GO was not reduced completely, but comparing with GO spectra, the C=O and C-O peak show low intensity in rGO_1. Then, after combining with NiFe LDH with hydrothermal treatment, the oxygen containing functional groups were almost removed from the composites, as shown

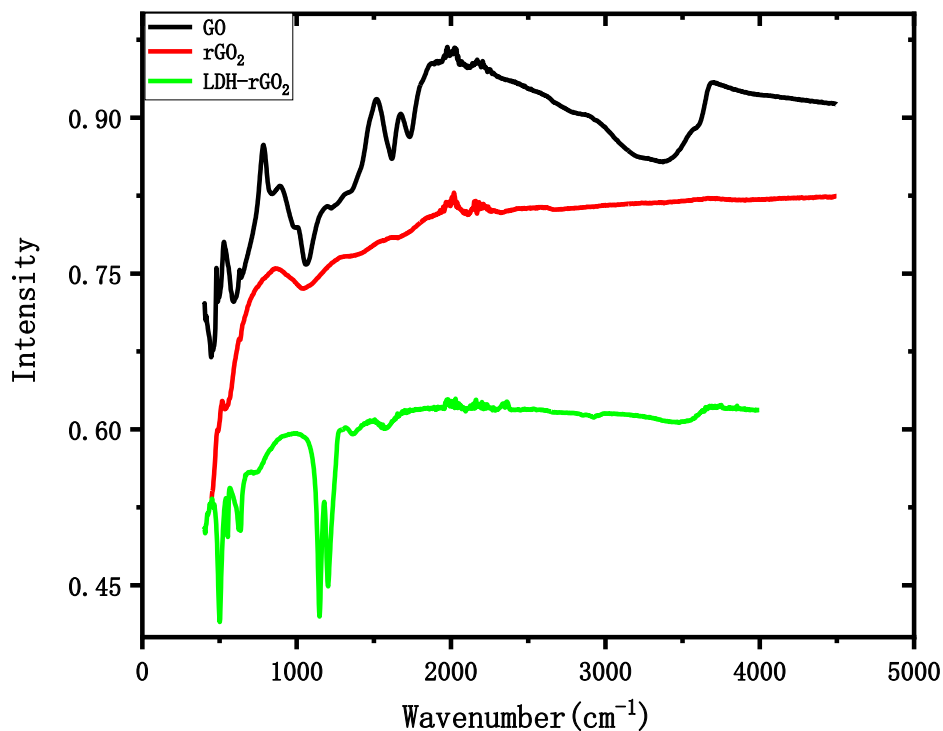in NiFe LDH-rGO₁ spectra. So we can state that the rGO was fully reduced after hydrothermal digestion.

Fig 21. FT-IR spectra of GO, rGO₂ and NiFe LDH-rGO₂

For hot water alkaline condition prepared rGO₂, the FTIR spectra showed the disappearance of oxygen content. As we expected, after combining with NiFe LDH by hydrothermal method, there were no conspicuous changes in oxygen containing functional groups, except the intensity of C-O groups get contracted and strengthened, which was quite different with hot water neutral condition prepared rGO₁. As we mentioned before, the rGO prepared by hot water in neutral condition was easy to restack and form an aggregation that may prevent the further reduction. As a result, there were some oxygen content left in rGO₁ samples. But by adding ammonia to adjust the pH value of the reaction

29

solution to 10 and to increase the negative surface charge of rGO the aggregation was prevented. Therefore, the rGO_2 can be fully reduced.
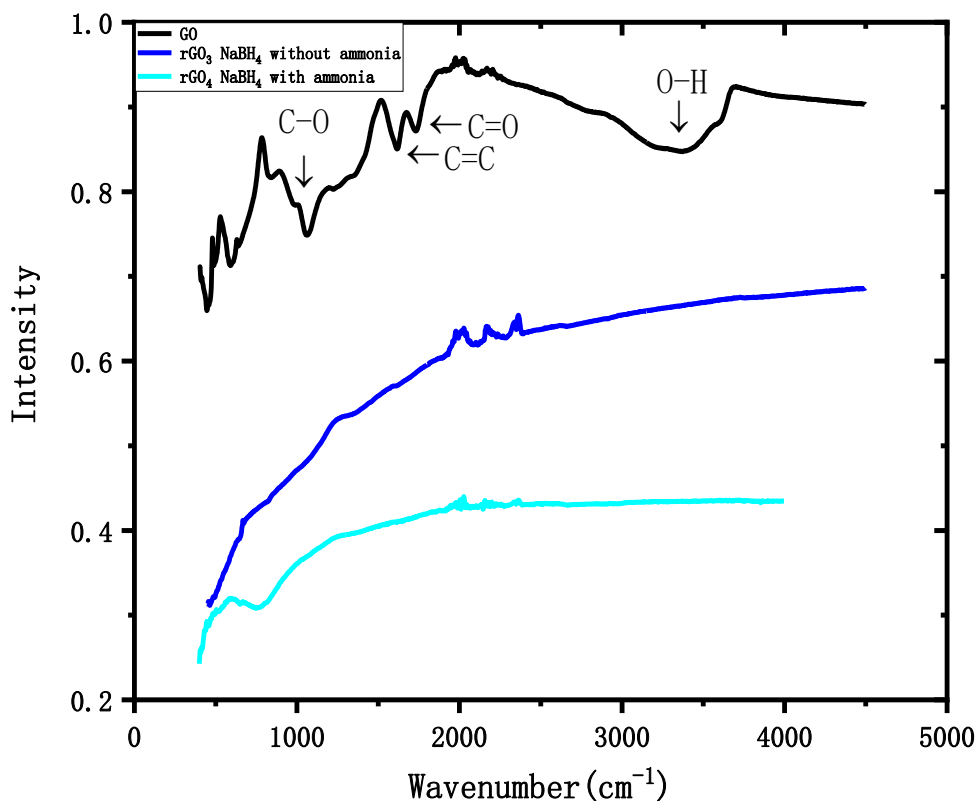

Fig 22. FT-IR spectra of GO, rGO_3 and rGO_4

Comparing with hot water prepared $rGO_{1,2}$, $NaBH_4$ reduced $rGO_{3,4}$ showed a better reduction activity on GO both in neutral and alkaline condition, as it showed in Figure 22. The FTIR spectra of $rGO_{3,4}$. there were no oxygen containing functional groups (C=O and C-O) in both alkaline and neutral condition prepared rGO samples. We can conclude that $NaBH_4$ worked as a reducing agent was superior than hot water for GO reduction and it can completely remove the oxygen content from rGO sample. Meanwhile, the effect of ammonia was not obvious on the reduction activity when the $NaBH_4$ was employed as a reducing agent for GO reduction.
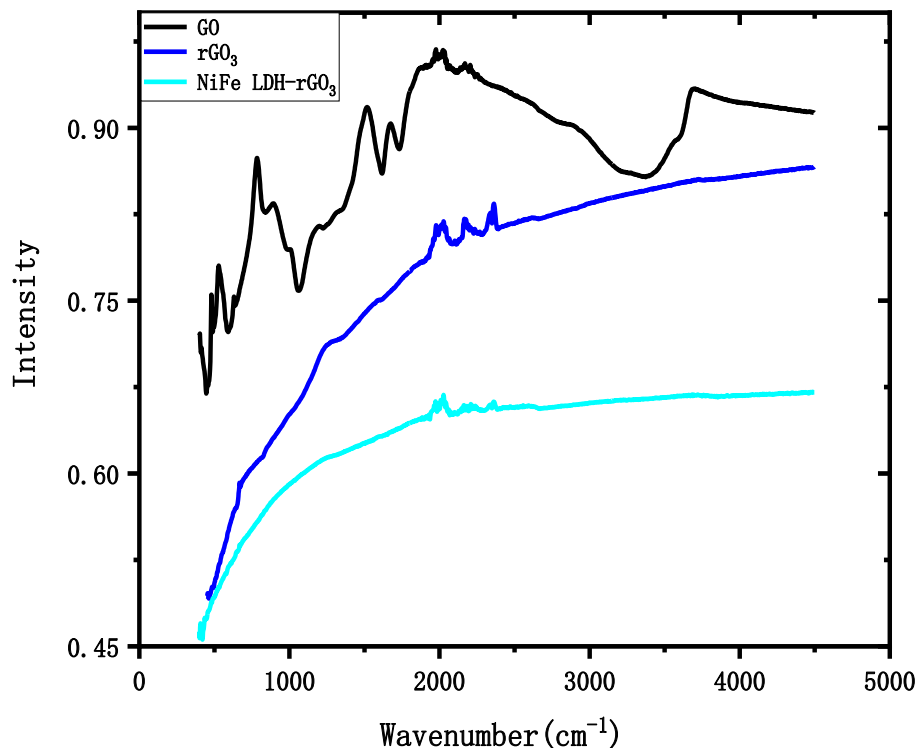
Fig 23. FT-IR spectra of GO, rGO$_3$ and LDH-rGO$_3$

The comparison of rGO$_3$ (NaBH$_4$ reduced without ammonia) and LDH-rGO$_3$ spectra is shown in Figure 23. From the graph, we can see, the spectrum of rGO$_3$ was flat and no conspicuous oxygen-containing chemical functional groups peaks. After the hydrothermal treatment, rGO$_3$ combined with LDH showed no changes in the spectrum. Therefore, we can conclude that the rGO$_3$ and LDH-rGO$_3$ composite were completely reduced. However, the C=C chemical functional groups band was also disappeared in both rGO$_3$ and LDH-rGO$_3$ composite spectra.

Similar results were obtained for rGO$_4$ and LDH-rGO$_4$ composite (Figure 24). the sharp band attributing to C=O chemical functional groups between 1600 cm^{-1} to 1650 cm^{-1} were completely disappeared in both rGO$_4$ and LDH-rGO$_4$ composite spectra. The other oxygen containing chemical functional groups C-O peaks and O-H peaks at 1055 cm^{-1} and 3400

cm^{-1} respectively were also disappeared in these two samples along with C=C functional groups.
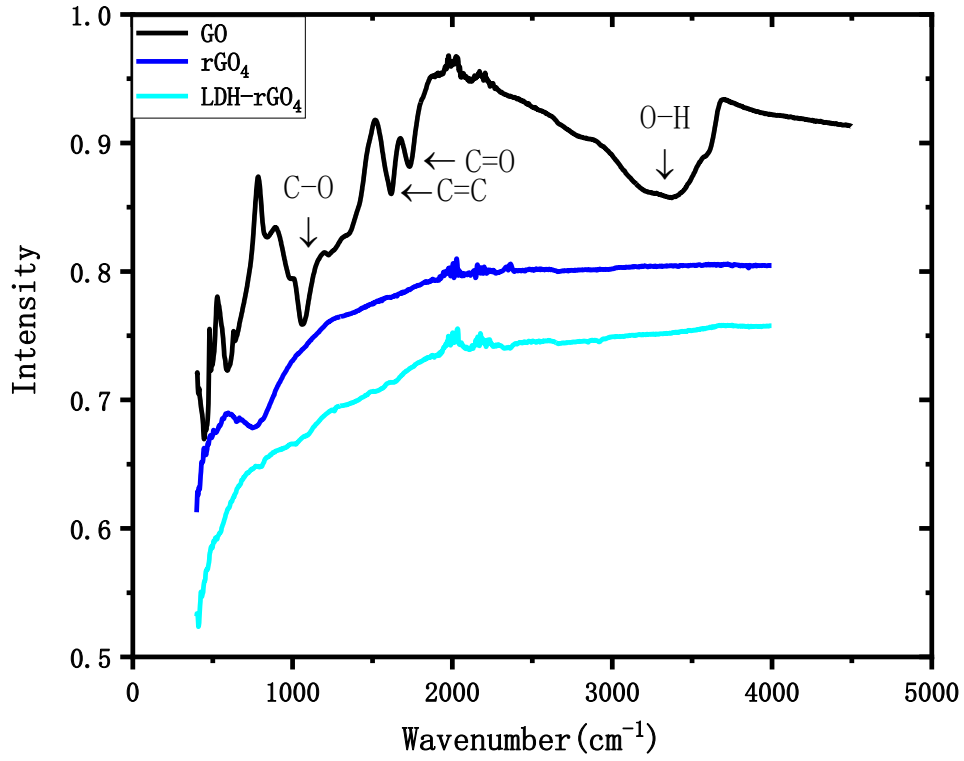

Fig 24. FT-IR spectra of GO, rGO$_4$and LDH-rGO$_4$

4.3. Electrocatalytic evaluation upon CO_2 conversion

In this work, the CO_2 reduction reaction took place in a three-electrode cell and cyclic voltammetry method was used to study the result of reduction reaction. The electrolyte used for the experiment was 0.1 M $TBAPF_6$ which was a wildly used organic electrolyte and dissolved in acetonitrile as electrolyte solution to saturate CO_2. The potential applied on the working electrode-GCE was firstly swept from lower vertex potential 0 V to upper vertex potential -2 V and then swept back to initial 0 V with a scan rate of 0.05 V/s to obtain a full cycle. The cyclic voltammograms of N_2 and CO_2 electro-reduction with and without the presence of NiFe LDH were showed in Figure 25. As we can see, the black curve (N_2 atmosphere) showed no current response, whereas the blank CO_2 started to get reduced when the overpotential was approximately -1.9 V (red curve). This large overpotential was attributed to CO_2 one electron reduction to overcome the barrier and form an intermediate $CO_2^{\cdot-}$. Whereas the cyclic voltammogram of the working electrode coated with NiFe LDH presented a lower reduction potential on CO_2 reduction, at around -1.6 V (green and blue curve). Therefore, we can infer that NiFe LDH have a positive effect on CO_2 electro-reduction.
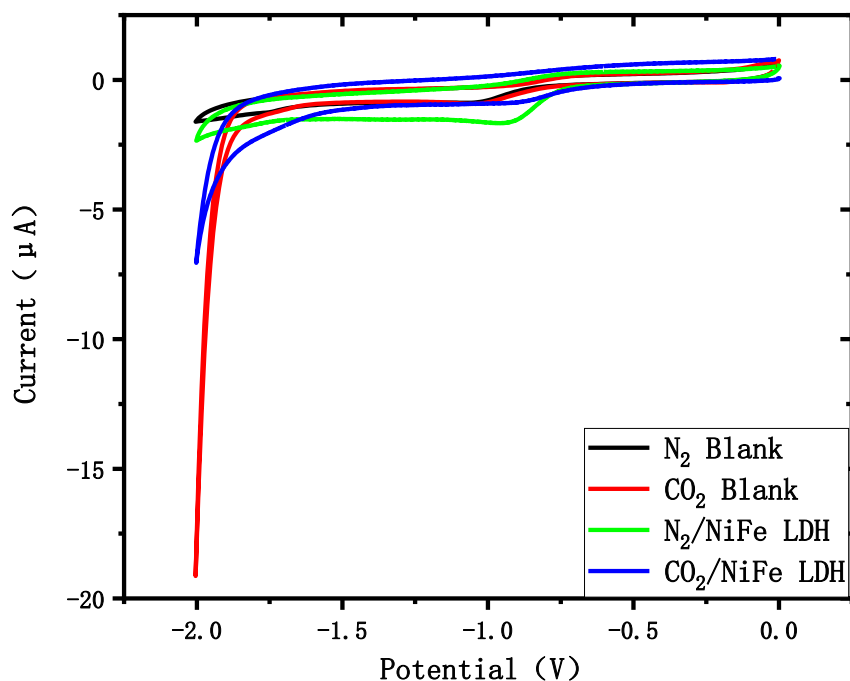
Fig 25. Cyclic voltammetry of bare and NiFe LDH coated electrode at N_2 and CO_2 atmosphere.

As mentioned before, because of the exceptional properties of rGO, we employed rGO as a support materials and combined it with NiFe LDH to enhance the electro-conductivity and specific surface areas of the composite and improve the catalytic activity of the composite on CO_2 electro-reduction. Figure 26 showed that the cyclic voltammogram of NiFe LDH-$rGO_{1,2}$ composites in the presence of N_2 and CO_2, where rGO_1 and rGO_2 was prepared with hot water in neutral and alkaline condition respectively. As we can see, the black curve presented the current against potential of LDH-rGO_1 composite at N_2 atmosphere (black curve) and it showed less current response (-3 μA). Then CO_2 was bubbled into the electrolyte solution for 15 minutes and current was measured against potential again (red curve).There is a clear difference in current response at -1.3 V was observed by comparing the black curve and red curve, that we can deduce that the reduction

potential of CO_2 was -1.3 V in the presence of NiFe LDH-rGO$_1$ composite,. Similar result was obtained for NiFe LDH-rGO$_2$ composite and the reduction potential of CO_2 was -1.3 V, but the latter showed high current response (-11 µA). At the same time, two reductive and oxidative peaks were observed at both N_2 and CO_2 atmosphere (green and blue curve). It can be attributed to the Ni^{2+} and Fe^{3+} ions reduction and oxidation process. As a result, we can conclude that the same CO_2 reduction potential was found for both composites, but NiFeLDH-rGO$_1$composite showed an high current response around -11µA against -7.5 µA of NiFe LDH-rGO$_2$ composite.
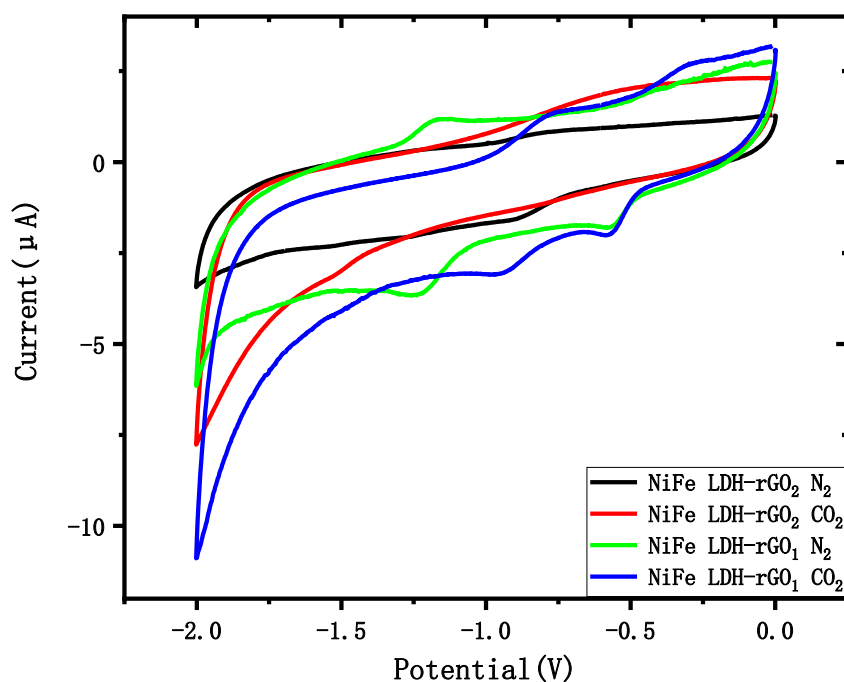

Fig 26 Cyclic voltammetry of NiFe LDH-rGO$_{1,2}$composites coated electrode at N_2 and CO_2 atmosphere.

The cyclic voltammogram of NiFe LDH-rGO$_{3,4}$ composites where rGO$_3$ and rGO$_4$ were prepared by $NaBH_4$ in neutral and alkaline condition was showed in Figure 27. The activity difference was observed at -1.5 V between black (N_2 atmosphere) and red curve (CO_2

atmosphere). Whereas the low reduction potential, and big current response was found in the presence of NiFe LDH-rGO$_3$ composite for CO_2 electro-reduction reaction. Thus, we can infer that rGO reduced by NaBH$_4$ in neutral condition presented a better catalytic activity enhancement of the composite on CO_2 electro-reduction than in alkaline condition prepared rGO.
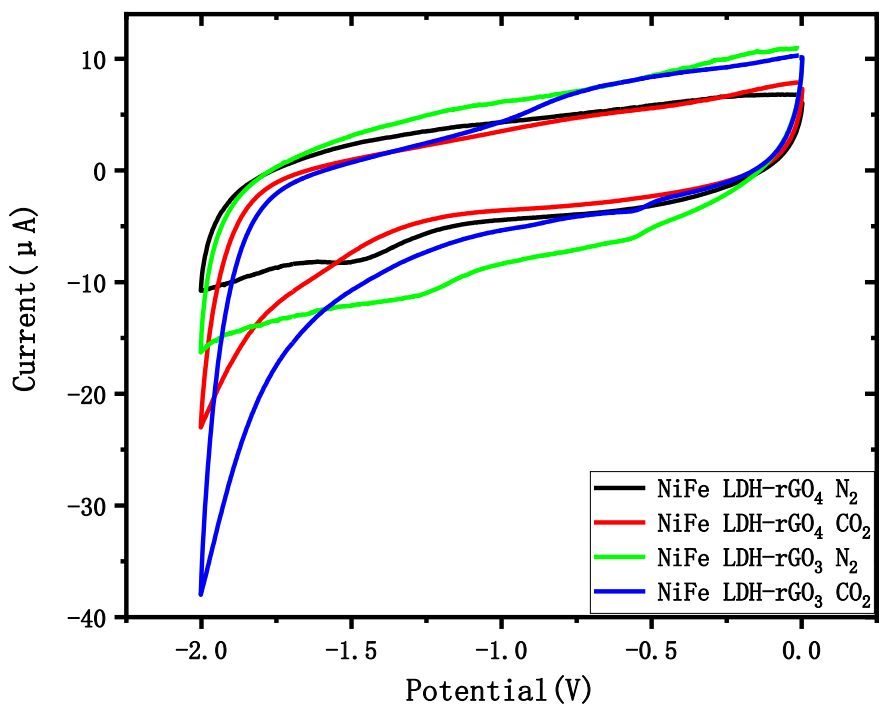

Fig 27 Cyclic voltammetry of NiFe LDH-rGO$_{3,4}$ composites coated electrode at N$_2$ and CO$_2$ atmosphere.

After comparing the NiFe LDH-rGO composites, where rGOs were synthesized by i) hot water and ii) NaBH$_4$ both in neutral and alkaline condition, We found that rGO prepared in neutral condition for both reduction methods improved the electro-conductivity and catalytic activity better than alkaline condition prepared rGO. Thus, we took out the neutral condition prepared samples-NiFe LDH-rGO$_{1,3}$ composites and comparing their CO$_2$

reduction effect with pure LDH. As shown in Figure 28, It was clear that the LDH-rGO₁ composite showed less reduction potential than (-1.3 V) than —pure LDH (-1.6 V). Although there were some fluctuations in the cyclic voltammogram of LDH-rGO₁ composite as mentioned before, we presumed it should be the metal ions redox process.
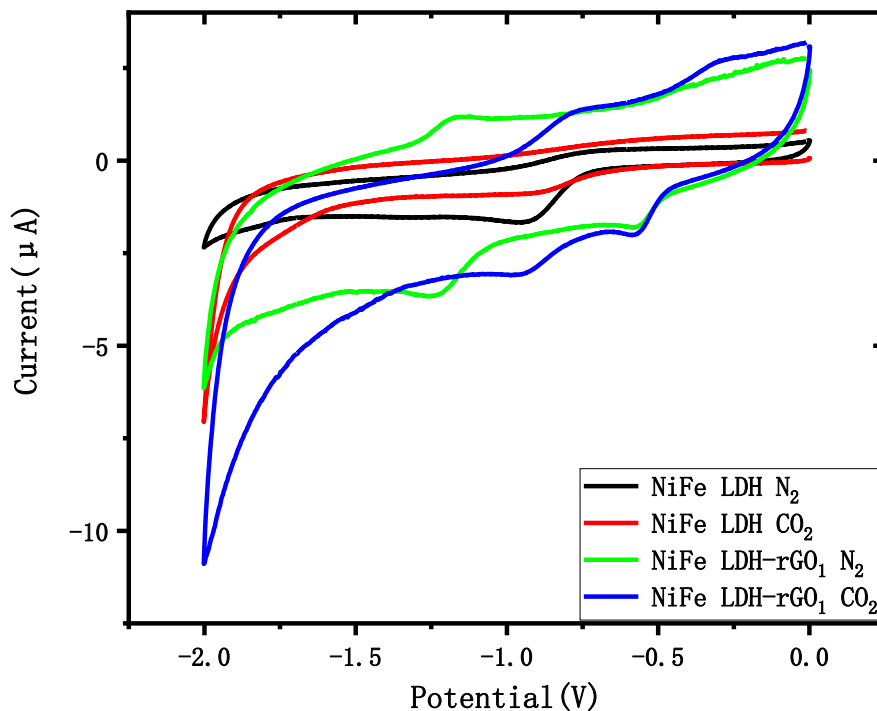

Fig 28. Cyclic voltammetry comparison between NiFe LDH-rGO₁ composite and pure NiFe LDH at N_2 and CO_2 atmosphere.

The comparison of CO_2 electro-reduction performance between NiFe LDH-rGO₃ composite and pure NiFe LDH was showed in Figure 29. a high current response was observed in the cyclic voltammogram of LDH-rGO₃ composite at CO_2 atmosphere, approximately -40 µA, it was 5 times bigger than that of LDH, most importantly, the composite showed a low reduction potential on CO_2 reduction (-1.3 V), whereas the reduction potential for pure LDH was found at -1.6 V. Consequently, we can conclude that

rGO prepared by NaBH$_4$ in neutral condition also showed an enhancement in electroconductivity and the catalytic performance of the composite on CO$_2$ electro-reduction.
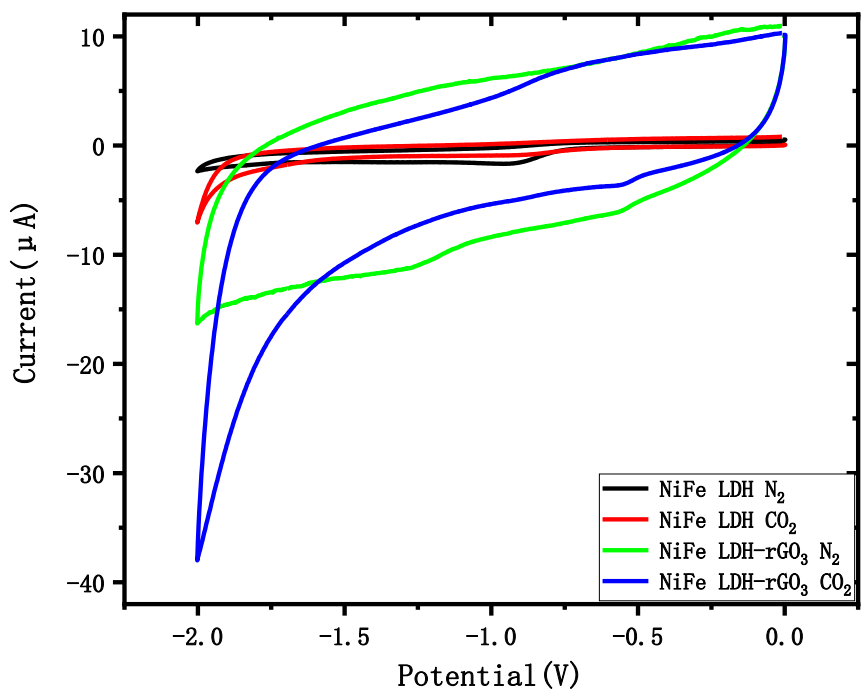

Fig 29. Cyclic voltammetry comparison between NiFe LDH-rGO$_3$ composite and pure NiFe LDH at N$_2$ and CO$_2$ atmosphere.

Further improvement has been carried out by changing the composition ratio between LDH and rGO$_1$ (prepared by hot water in neutral condition) during LDH-rGO$_1$composite preparation process. Firstly, two composites with different composition ratios (50%-50% and 90%-10%) between LDH and rGO$_1$ were prepared with hydrothermal method in same condition. The cyclic voltammograms were showed in Figure 30, the composite consisted of 90% LDH and 10% rGO$_1$ showed a low current response, approximately -7 μA and the CO$_2$ reduction potential was -1.5 V. whereas the other composite composing of 50% LDH and 50% rGO$_1$, represented a better catalytic performance on CO$_2$ reduction, where the

CO_2 reduction potential was -1.3 V and a big current response was observed (-11 µA). Thus, we can presume that the LDH-rGO$_1$composite with 50%-50% composition ratio had a better catalytic activity on CO_2 reduction than the one with 90%-10% composition ratio.
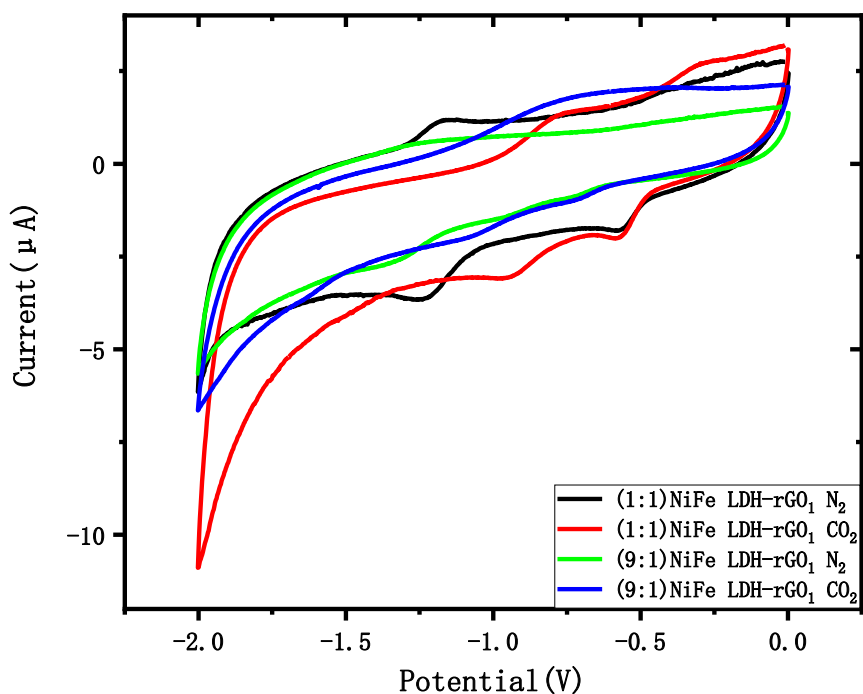

Fig 30. Effect of composition ratio between LDH and rGO (1:1 Vs 9:1) on CO_2 electro-reduction.

Thus, we compared effect of the composites with different composition ratio between rGO and LDH and found the composite with 50% rGO and 50% LDH performed better than the other composite on CO_2 electro-reduction. Now, in this experiment, a composite consisting of 75% LDH and 25% rGO$_1$ was synthesized and investigated on CO_2 electro-reduction reaction. Figure 31 showed the comparison of LDH-rGO$_1$ composites with different composition ratios (50%-50% and 75%-25%) on CO_2electro-reduction. The activity difference was observed between green and blue curve at around -1.3 V. so we can infer that the CO_2 reduction potential was -1.3 V at the presence of LDH-rGO$_1$ composite with

75%-25% composition ratio. Similar CO_2 reduction point was found for the composite with 50%-50% composition ratio. However, the former composite showed big current response, approximately -25 µA.
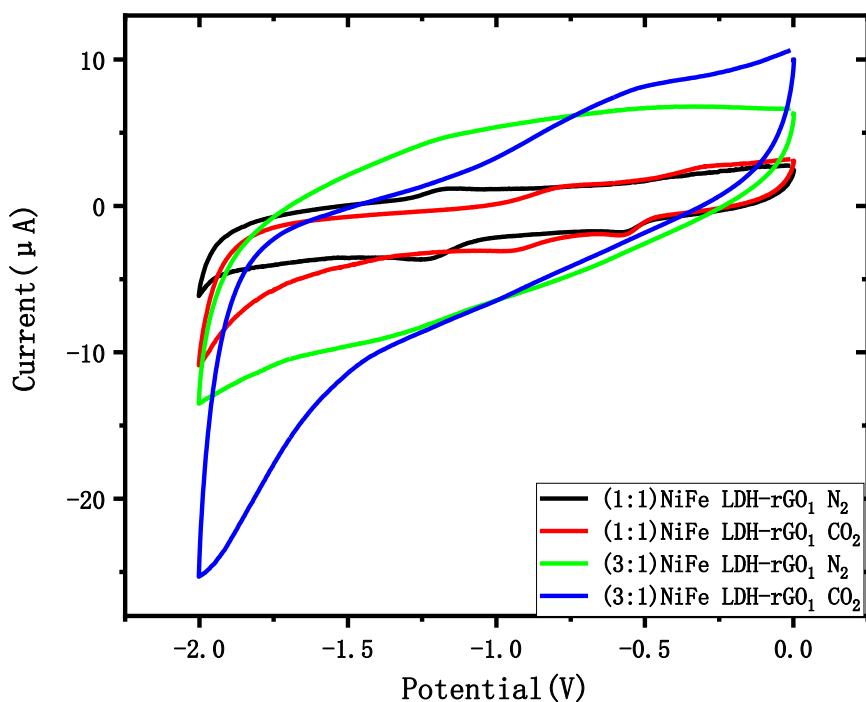
Fig 4.31. Effect of composition ratio between LDH and rGO (1:1 Vs 3:1) on CO_2 electro-reduction.

In our previous work, we also employed layered double oxides (LDOs) for CO_2 electro-reduction and found it showed a positive catalytic activity. So in this thesis, we combined NiFe LDO with rGO_1 (prepared by hot water in neutral condition) by hydrothermal method to form a LDO based composite for electro-catalysis of CO_2 reduction. Figure 32 represented the comparison of LDH-based composite and LDO-based composite on CO_2 electro-reduction.. As we can see, there was no obvious activity difference between green and blue curve (LDO N_2 & CO_2), whereas LDH-based composite material conspicuous

current difference at -1.3 V. Thus, we can conclude rGO_1 improved the catalytic activity of LDH-based composite better than LDO-based composite.

Fig 32. Cyclic voltammetry of NiFe LDH-rGO_1composite and NiFe LDO-rGO_1 composite coated electrode at N_2 and CO_2 atmosphere.

Besides, we also combined LDO with rGO_3 (prepared using $NaBH_4$ in neutral condition) to compare the catalytic activity with LDH-rGO_3 composite on CO_2 electro-reduction. The result was showed in Figure 33. The CO_2 reduction potential was found at -1.5 V and -1.3 V for LDH and LDO composites respectively. LDO composite material (blue curve) was showing an improved activity than LDH composite as the reduction occurs at lower potential. Also, calcination process has changed the electrical property of the material leaving LDO with more capacitance current (based on the curve area).
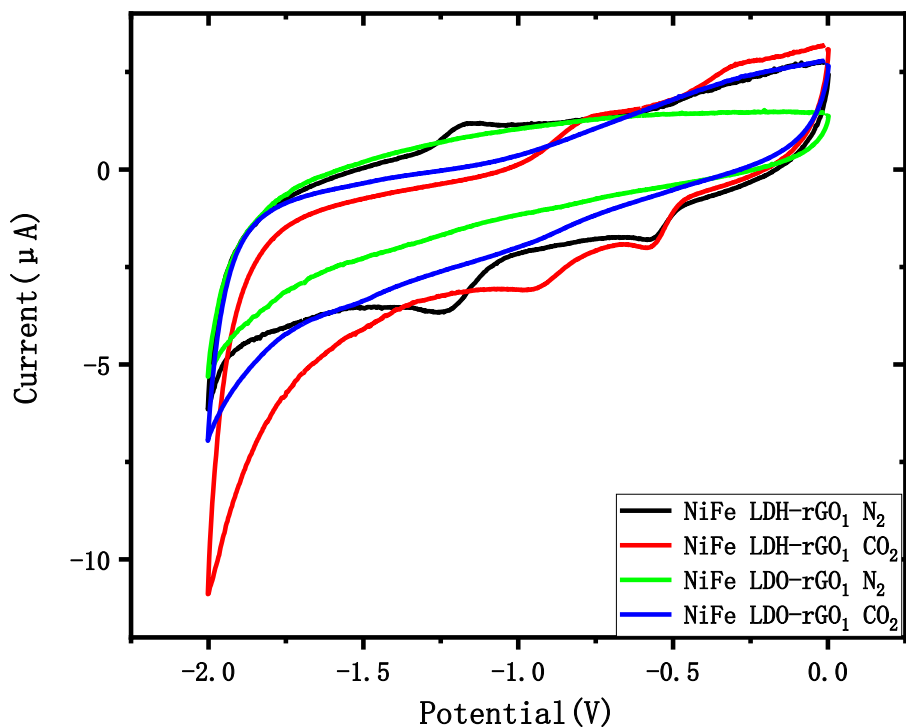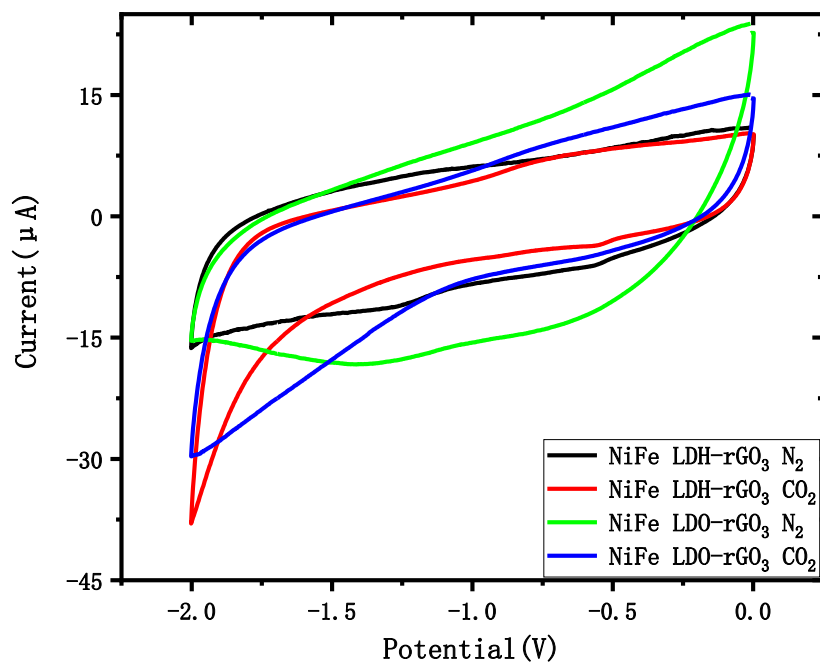
Fig 33. Cyclic voltammetry of NiFe LDH-rGO₃ composite and NiFe LDO-rGO₃ composite coated electrode at N_2 and CO_2 atmosphere.

5. Discussion

In this work, we investigated LDH and LDH-rGO composites, which were prepared by different methods, as catalysts for CO_2 electro-reduction. As we expected that rGO would improve the electro-conductivity and catalytic reactivity of the composite, the results were in alignment with our hypothesis. The essence of high electrical conductivity property was attributed to the sp^2 hybridization structure in graphene. However, in some cases, FI-TR spectrum of rGO, showed that the intensity of C=C was not strengthened after the reduction reaction. Some of composite samples even showed a diminishment of C=C groups after hydrothermal treatment. Further investigation needed to verify this problem.

The electrolyte and solvent we used for CO_2 electro-reduction reaction was immutable, it was only TBAPF6 and acetonitrile. There were no proton precursors in this three electrodes cell system. As a result, in the experiment, there was only one certain reduction route where CO_2 one electron reduction took place to form $CO_2^{\bullet-}$ and finally yielding CO. It was possible to utilize some inorganic electrolytes solution or introduce some proton precursors such as water, hydrogen chloride in the system, which will has a big impact on the reduction reaction. As a result, there may be some other reaction routes and other value-added carbon compounds with diverse valence states may yield, and the CO_2 reduction potential may change at the same time. In addition our attention only focused on whether the as-synthesized composites can improve the efficiency of CO_2 electro-reduction and present a low CO_2 reduction potential and high current response. Hence we did not pay much attention on the yielded products and efficiency of conversion. For instance, besides the CO, if there were any other products produced during the reduction reaction or not and how was CO_2 conversion percentage etc. But it was obvious that the time was limited for the project. Nevertheless, the results presented are certainly an exciting area and more attention/investigation needed in future.

As mentioned before, CO_2 one electron reduction took place where the overpotential applied on the bare working electrode was over -1.9 V in three electrodes cell system. According to the results, by introducing NiFe LDH-rGO composite as a catalyst to compensate the energy barrier of CO_2 reduction reaction, the overpotential was considerably reduced. Although it was in initial laboratories phase, but with great prospects,. with more and more scientist's participation and devotion, this technology can be put into practice to reduce CO_2 content in the atmosphere with less energy consumption and alleviate the greenhouse effect in the near future.

6 Conclusion

In this work, we synthesized different types of NiFe LDH-rGO composites by combining NiFe LDH with rGO that was prepared in both alkaline and neutral condition using i) Hot water ii) $NaBH_4$. These composites were all used for CO_2 electro-reduction. According to the results, we found the neutral condition for rGO synthesis showed better results than alkali condition as those samples ($rGO_{1,3}$) showed less reduction potential and more current response on CO_2 electro-reduction reaction. As we expected, LDH-rGO composite was performing better than pure LDH on CO_2 electro-reduction. The CO_2 reduction potential was found to be -1.3 V as against pure LDH, i.e. -1.6 V. Thus, rGO improves the electro-conductivity of the composite and catalytic activity. Furthermore, we prepared NiFe LDH-rGO composite with different composition ratios for CO_2 electro-reduction and the best ratio was 3:1 (75% LDH-25% rGO). Finally, we also compared LDH-based composite and LDO-based composite. The results revealed that LDH-rGO(water) was more active than LDO-rGO(water), whereas LDO-rGO$_{(NaBH4)}$ was more active than LDH-rGO$_{(NaBH4)}$ in CO_2 electro-reduction.

Reference

[1] L. A. Arias, E. Rivas, F. Santamaria and V. Hernandez. A Review and Analysis of Trends Related to Demand Response. *Energies* 2018,11, 1617.

[2] Climate Change 2014: Mitigation of Climate Change. Retrieved from www.ipcc.ch/report/ar5/wg3.

[3] Climate Change 2014: Mitigation of Climate Change. Retrieved from https://www.epa.gov/ghgemissions/global-greenhouse-gas-emissions-data.

[4] Wang, W., Wang, S.P., Ma, X.B., and Gong, J.L. (2011). Recent advances in catalytic hydrogenation of carbon dioxide. Chem. Soc. Rev. 40, 3703–3727.

[5] P. Sipos, I. Pálinkó, As-prepared and intercalated layered double hydroxides of the hydrocalumite type as efficient catalysts in various reactions, Catal. Today 306 (2018) 32-41.

[6] Y. Guo, Z. Zhu, Y. Qiu, J. Zhao, Enhanced adsorption of acid brown 14 dye on calcined Mg/Fe layered double hydroxide with memory effect, Chem. Eng. J. 219 (2013) 69-77.

[7] J. Xu, Y. Song, Q. Tan, L. Jiang, Chloride absorption by nitrate, nitrite and aminobenzoate intercalated layered double hydroxides, J. Mater. Sci. 52 (2017) 5908-5916.

[8] D.G. Evans, R.C.T. Slade, Structural Aspects of Layered Double Hydroxides, Struct. Bond. 119 (2006) 1–87.

[9] Evans, David G.; Slade, Robert C. T. "Structural aspects of layered double hydroxides" Structure and Bonding 2006, vol. 119, 1-87.

[10] "IMA Nomenclature Report".

[11] M.V. Bukhtiyarova, A review on effect of synthesis conditions on the formation of layered double hydroxides, Journal of Solid State Chemistry, (2019) 0022-4596.

[12] P.P. Huang, C.Y. Cao, F. Wei, Y.B. Sun, W.G. Song, MgAl layered double hydroxides with chlorine and carbonate ions as interlayer anions for removal of arsenic and fluoride ions in water, RCS Adv., 5 (2015) 10412-10417.

[13] H.S. Panda, R. Srivastava, D. Bahadur, Synthesis and in situ mechanism of nuclei

growth oflayered double hydroxides, Bull. Mater. Sci. 34 (2011) 1599-1604.

[14] L. Zhang, J. Zhu, X. Jiang, D.G. Evans, F. Li, Influence of nature of precursors on the formation and structure of Cu–Ni–Cr mixed oxides from layered double hydroxides, J. Phys. Chem. Solids 67 (2006) 1678-1686.

[15] M. Ogawa, H. Kaiho, Homogeneous precipitation of uniform hydrotalcite particles, Langmuir 18 (2002) 4240-4242.

[16] T. Lopez, P. Bosch, E. Ramos, R. Gomez, O. Novaro, D. Acosta, F. Figueras, Synthesis and characterization of sol-gel hydrotalcites. Structure and texture, Langmuir 12 (1996) 189-192.

[17] M. Jitianu, D.C. Gunness, D.E. Aboagye, M. Zaharescu, A. Jitianu, Nanosized Ni–Al layered double hydroxides—Structural characterization, Mater. Res. Bull. 48 (2013) 1864-1873.

[18] Flegler, A., Müssig, S., Prieschl, J., Mandel, K. &Sextl, G. Towards core-shell bifunctional catalyst particles for aqueous metal-air batteries: NiFe-layered double hydroxide nanoparticle coatings on g-MnO$_2$ microparticles. Electrochimica. Acta 231, 216–222 (2017).

[19] Xu, Z. P. et al. Subcellular compartment targeting of layered double hydroxide nanoparticles. J. Control Rel. 130, 86–94 (2008).

[20] Fan, G., Li, F., Evans, D. G. & Duan, X. Catalytic applications of layered double hydroxides: recent advances and perspectives. Chem. Soc. Rev. 43, 7040–7066 (2014).

[21] Lu, Y. et al. Highly sensitive nonenzymatic glucose sensor based on 3D ultrathin NiFe layered double hydroxide nanosheets. Electroanalysis 29, 1755–1761 (2017).

[22] A.K. Geim, K.S. Novoselov, Detection of individual gas molecules adsorbed on graphene, Nat. Mater. 6 (2007) 183–191.

[23] J.H. Chen, C. Jang, S.D. Xiao, M. Ishigami, M.S. Fuhrer, Intrinsic and extrinsic performance limits of graphene devices on SiO$_2$, Nat. Nanotechnol. 3 (2008).

[24] J.H. Seol, I. Jo, A.L. Moore, L. Lindsay, Z.H. Aitken, M.T. Pettes, X.S. Li, Z. Yao, R. Huang, D. Broido, N. Mingo, R.S. Ruoff, L. Shi, Two-dimensional phonon transport in supported graphene, Science 328 (2010) 213–216.

[25] Lee, C., Wei, X.D., Kysar, J.W., Hone, J.: Measurement of the elastic properties and intrinsic strength of monolayer graphene. Science 321, 385–388 (2008).doi:10.1126/science.1157996

[26] C. Lee, X.D. Wei, J.W. Kysar, J. Hone, Measurement of the elastic properties and intrinsic strength of monolayer graphene, Science 321 (2008) 385–388. 206–209.

[27] Md. SajibulAlamBhuyan, et al, Synthesis of graphene. Int Nano Lett (2016) 6:65–83. Doi: 10.1007/s40089-015-0176-1.

[28] Joshi, R. K. et al. Precise and ultrafast molecular sieving through graphene oxide membranes.Science343, 752–754 (2014).

[29] Su, Y. et al. Impermeable barrier films and protective coatings based on reduced graphene oxide. Nat. Commun.5, 3906 (2014).

[30] Yadav, R., Subhash, A., Chemmenchery, N. & Kandasubramanian, B. Graphene and graphene oxide for fuel cell technology. Ind. Eng. Chem. Res.57, 9333–9350 (2018).

[31] Farooqui, U., Ahmad, A. & Hamid, N. Graphene oxide: a promising membrane material for fuel cells. Renew. Sustain. Energy Rev.82, 714–733 (2018).

[32] Jung, H. S. et al. Nanographene Oxide–Hyaluronic Acid Conjugate for Photothermal Ablation Therapy of Skin Cancer. ACS Nano, 8(1), 260-268.

[33] Sun, X. et al (2008). Nano-Graphene Oxide for Cellular Imaging and Drug Delivery. Nano Res1, 203–212.

[34] Chen, C.Y. et al. Graphene oxide: a novel acid catalyst for the synthesis of 2,5-dimethyl-N-phenyl pyrrole by the Paal–Knorr condensation New Carbon Materials, 2017, 32(2): 160-167.

[35] R. Bhargava, S. Khan, M. M. N. Ansari, and N. Ahmad, Green synthesis approach for the reduction of graphene oxide by using glucose. AIP Conference Proceedings 2115,

030075 (2019).

[36] Wang S, Ang PK, Wang Z, Tang ALL, Thong JTL, Loh KP. High mobility, printable, and solution-processed graphene electronics. Nano Letters. 2010;10:92.

[37] A.Velasco and et al. Recent trends in graphene supercapacitors: from large area to micro supercapacitors. Sustainable Energy Fuels,2021,5,1235.

[38] D. Pan, S. Wang, B. Zhao, M. Wu, H. Zhang, Y. Wang, Z. Jiao, Chem. Mater. 21 (2009) 3136.

[39] El-Kady, M., Shao, Y. &Kaner, R. Graphene for batteries, supercapacitors and beyond. Nat Rev Mater 1, 16033 (2016).

[40] M. Obodo, et al., 2019. Introductory Chapter: Graphene and Its Applications, in: .. doi:10.5772/intechopen.86023.

[41] Y.W. Li, H.B Su, S.H. Chan, Q. Sun, CO_2 Electroreduction Performance of Transition Metal Dimers Supported on Graphene: A Theoretical Study *ACS Catal.* 2015, 5, 11, 6658–6664.

[42] Phan, T.H., Banjac, K., Cometto, F.P., Dattila, F., GarcíA-Muelas, R., Lopez, N., Lingenfelder, M., 2020. Tracking the Potential-Controlled Synthesis of Cu-Nanocuboids and Graphene-Covered Cu-Nanocuboids Under Operando CO2 Electroreduction. doi:10.26434/chemrxiv.13198481.v1.

[43]. R.J. Lim, M. Xie, M.A. Sk, J.-M. Lee, A. Fisher, X. Wang, and K.H. Lim, (2014) Catalysis. Today, 233:169–180.

[44]. R. Schlögl, (2015) Angew. Chemie Int. Ed., 54:3465–3520.

[45]. J. Qiao, Y. Liu, F. Hong, and J. Zhang, (2014) Chem. Soc. Rev., 43:631–675.

[46]. J. Albo, M. Alvarez-Guerra, P. Castaño, and A. Irabien, (2015) Green Chem., 17:2304–2324 .

[47] Benson, Eric E.; Kubiak, Clifford P.; Sathrum, Aaron J.; Smieja, Jonathan M. (2009). "Electrocatalytic and homogeneous approaches to conversion of CO2 to liquid fuels". Chem. Soc. Rev. 38 (1): 89–99. doi:10.1039/b804323j. PMID 19088968.

[48]T. -J.Wan,S.-M.Shen,A.Bandyopadhyay,C.-M.Shu,Sep.Purif.Technol.2012,94,87–91

[49] J. Hawecker, J. M. Lehn and R. Ziessel, J. Chem. Soc., Chem. Commun., 1984, 328–330.

[50] Gu, J.; Hsu, C. S.; Bai, L.; Chen, H. M.; Hu, X. Atomically Dispersed Fe^{3+} Sites Catalyze Efficient CO_2 Electroreduction to CO. Science (Washington, DC, U. S.) 2019, 364 (6445), 1091−1094.

[51] M. Le, M. Ren, Z. Zhang, P. T. Sprunger, R. L. Kurtz and J. C. Flake, J. Electrochem. Soc., 2011, 158, E45–E49.

[52] Y. H. Chen, C. W. Li and M. W. Kanan, J. Am. Chem. Soc., 2012, 134, 19969–19972.

[53] R. Aydin and F. Koleli, Synth. Met., 2004, 144, 75–80. 353 G. Seshadri, C. Lin and A. B. Bocarsly, J. Electroanal. Chem., 1994, 372, 145–150.

[54] G. Seshadri, C. Lin and A. B. Bocarsly, J. Electroanal. Chem., 1994, 372, 145–150.

[55] K. Sugimura, S. Kuwabata and H. Yoneyama, J. Am. Chem. Soc., 1989, 111, 2361–2362.

[56] Naveed Altaf, Shuyu Liang, Liang Huang and Qiang Wang. Electro-derived $Cu-Cu_2O$ nanocluster from LDH for stable and selective C_2 hydrocarbons production from CO_2electrochemical reduction. Journal of Energy Chemistry48, 169 (2020).

[57] S. Iguchi and et al. .Investigation of the electrochemical and photoelectrochemical properties of Ni–Al LDH photocatalysts. Phys.Chem.Chem.Phys.,2016,18,1381.

[58] N. Altaf, S. Liang, L. Huang and Q. Wang, Journal of Energy Chemistry 48, 169 (2020).

[59] S. Kawamura, N. Ahmed, G. Carja, Y. Izumi. Photocatalytic Conversion of Carbon Dioxide Using Zn–Cu–Ga Layered Double Hydroxides Assembled with Cu Phthalocyanine: Cu in Contact with Gaseous Reactant is Needed for Methanol Generation. Oil & Gas Science and Technology - Revue d'IFP Energies nouvelles, InstitutFrançais du Pétrole, 2015, 70 (5), pp.841-852.

[60] M. Flores-Floresa and et al. Photocatalytic CO_2 conversion by MgAl layered double

hydroxides: Effect of Mg^{2+} precursor and microwave irradiation time. Journal of Photochemistry & Photobiology A: Chemistry 363 (2018) 68–73.

[61] D. Vasudevan, Performance and Characterization Studies of Reduced Graphene Oxides Aqua Nanofluids for a Pool Boiling Surface. International Journal of Thermophysics (2020) 41:74,